materials

MDPI

Review

Probabilistic Analysis of Composite Materials with Hyper-Elastic Components

Marcin Kamiński * and Damian Sokołowski

Department of Structural Mechanics, Faculty of Civil Engineering, Architecture & Environmental Engineering, Łódź University of Technology, Al. Politechniki 6, 90-924 Lodz, Poland
* Correspondence: marcin.kaminski@p.lodz.pl

Abstract: This work is a comprehensive literature overview in the area of probabilistic methods related to composite materials with components exhibiting hyper-elastic constitutive behavior. A practical area of potential applications is seen to be rubber, rubber-like, or even rubber-based heterogeneous media, which have a huge importance in civil, mechanical, environmental, and aerospace engineering. The overview proposed and related discussion starts with some general introductory remarks and a general overview of the theories and methods of hyper-elastic material with a special emphasis on the recent progress. Further, a detailed review of the current trends in probabilistic methods is provided, which is followed by a literature perspective on the theoretical, experimental, and numerical treatments of interphase composites. The most important part of this work is a discussion of the up-to-date methods and works that used the homogenization method and effective medium analysis. There is a specific focus on random composites with and without any interface defects, but the approaches recalled here may also serve as well in sensitivity analysis and optimization studies. This discussion may be especially helpful in all engineering analyses and models related to the reliability of elastomers, whose applicability range, which includes energy absorbers, automotive details, sportswear, and the elements of water supply networks, is still increasing, as well as areas where a stochastic response is the basis of some limit functions that are fundamental for such composites in structural health monitoring.

Keywords: composites; hyper-elasticity; homogenization; probabilistic methods; interface defects; rubber-like materials

Citation: Kamiński, M.; Sokołowski, D. Probabilistic Analysis of Composite Materials with Hyper-Elastic Components. *Materials* **2022**, *15*, 8878. https://doi.org/10.3390/ma15248878

Academic Editor: Michal Sedlačík

Received: 11 November 2022
Accepted: 7 December 2022
Published: 12 December 2022

1. Introductory Remarks

The computational analysis of materials is now standard and decisive for the design of contemporary appliances, mechanical parts, and bearing systems that are made of both homogeneous and heterogeneous (composite) materials. It is especially remarkable in the area of polymeric materials [1] that are reinforced or filled with some other specific micro-injections or nano-particles [2–5]. Such materials modeling needs a specific approach that is most frequently based upon macro-modeling that is linked with a calculation of the overall properties [6]; nevertheless, it may demand precise experimentally verified knowledge concerning the nano-mechanics of the reinforcements [7]. There is no doubt that numerical simulation changed the entire design process by supplementing the traditional cycle of conceptualizing and laboratory testing with various modeling tools, including sensitivity analyses [8], stochastic models [9] that include various nonlinearities [10], accounting for the anisotropy of fillers [11], atomistic modeling [12], and multiscale approaches [13], finally leading to reliability assessments [14]. It cuts down the design time and provides tools for a very optimized or complex solution that is unavailable when using even a very advanced analytical approach. All computations are based on constitutive models of materials, which involves defining their behavior under different

mechanical, thermal [15], electrical [16], magnetic, and coupled [17] conditions. They are well-defined for relatively simple continua [18–20] but are still challenging for composites outside of the elastic region. In this review, the hyper-elastic response of a complex continuum is studied. It is highly useful for predicting the behavior of rubber-like composites with a polymeric matrix. Their main strengths include their ease of usage and calibration, computational efficiency, and flexibility of usage and accessibility in commercial codes. They could also be quite easily augmented to capture hysteresis in cyclic loading. Applications of various hyper-elastic constitutive models range from the tire industry to biological tissues, such as human arteries [21] and polymers, and include civil engineering, where such materials are applied as vibration dampers and protection.

This review work consists of five sections, starting with a retrospective look into hyper-elastic materials and their constitutive models. Then, a relatively short description and literature overview are given related to the probabilistic methods that are available in modern engineering. The next part is devoted to the characterization of interphases and interface defects that are inherent in composite materials. Further, multiscale models of composite materials and the additional numerical simulations are briefly characterized, together with their recent advances. The key milestones and very recent ideas in the homogenization method end the entire review.

2. Hyper-Elastic Materials

An early motivation for the theoretical formulation of hyper-elastic materials was the lack of existence of large-strain models capturing deformations that accounted for their non-linearity above an infinitesimal level. Such materials can deform significantly and nonlinearly upon loading without breaking and then return to their initial configuration. Such rubber elasticity is achieved due to very flexible long-chain molecules and a three-dimensional network structure that is formed via cross-linking or some entanglements between molecules. This behavior characterizes a wide range of continua, including rubber-like materials, polymers [22], and elastomers [23]. Its implementation in the finite element framework requires two important ingredients to solve the given boundary value problem. They are the stress tensor and the consistent fourth-order tangent operator; the latter is the result of linearization of the former rubber-like materials, which are generally modeled as homogeneous, isotropic, incompressible or nearly incompressible, geometrically and physically nonlinear, hyper- or visco-elastic solids [24–28] and visco-plastic solids [29]. Their models are commonly supported by experimental data. The most common tests involve uniaxial tension, biaxial tension, and pure shear. Some models also consider aging [30,31], the Mullins effect [32–34], hysteresis [35], or the failure of rubber-like materials [36,37]. Hyper-elastic models are reviewed in this work and their theoretical introduction is available, for example, in [38–41], whereas some numerical illustrations are contained in [42–45]. Let us recall the basic concepts for hyper-elastic constitutive models, which can be generally divided into three essentially different categories: phenomenological models [46,47], micromechanical approaches, and constitutive theories obtained with the use of the artificial neural networks (ANNs [48–52]). They are all presented graphically in Figures 1–4, respectively.

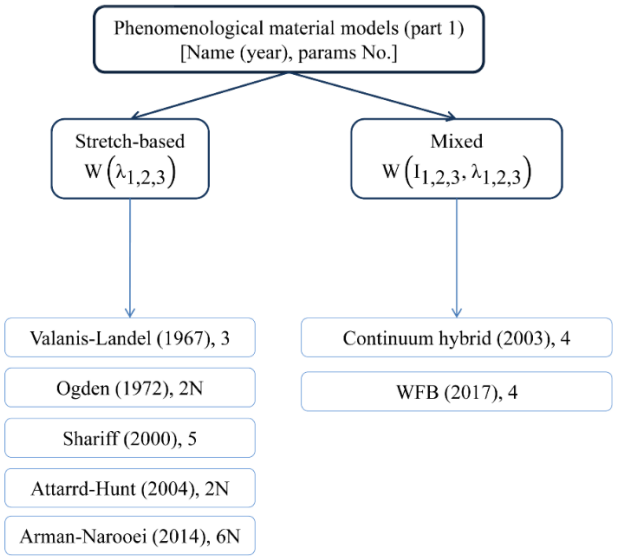

Figure 1. Different phenomenological models of hyper-elastic materials (part 1).

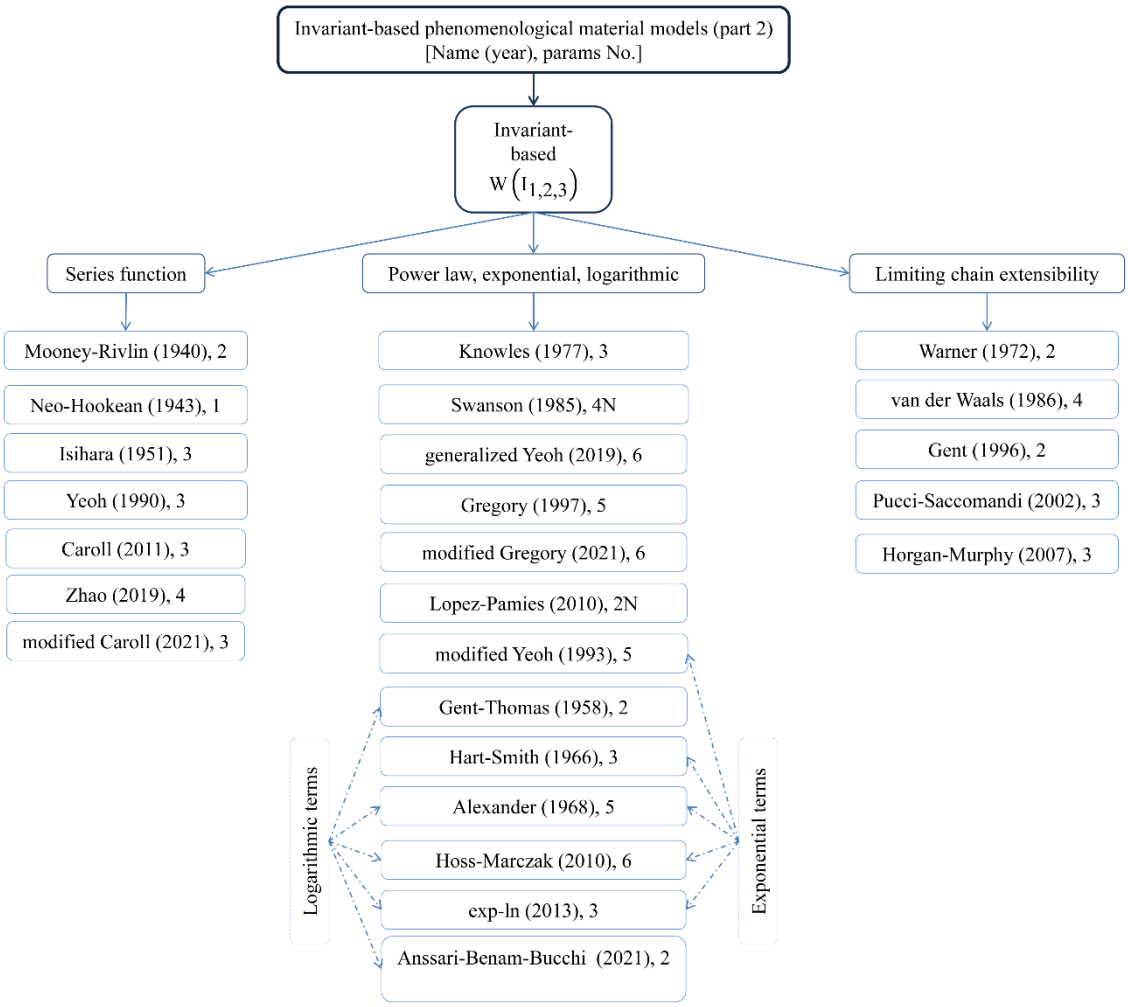

Figure 2. Different phenomenological models of hyper-elastic materials (part 2).

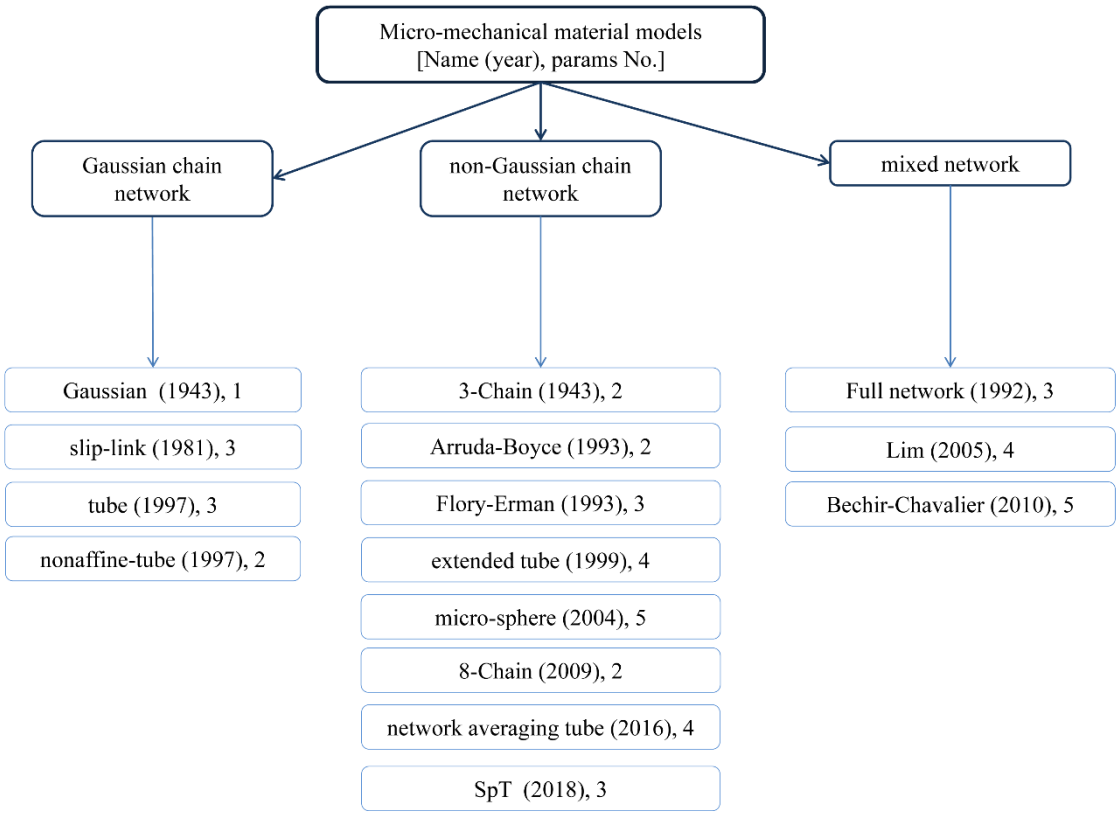

Figure 3. Different micromechanical models of hyper-elastic materials.

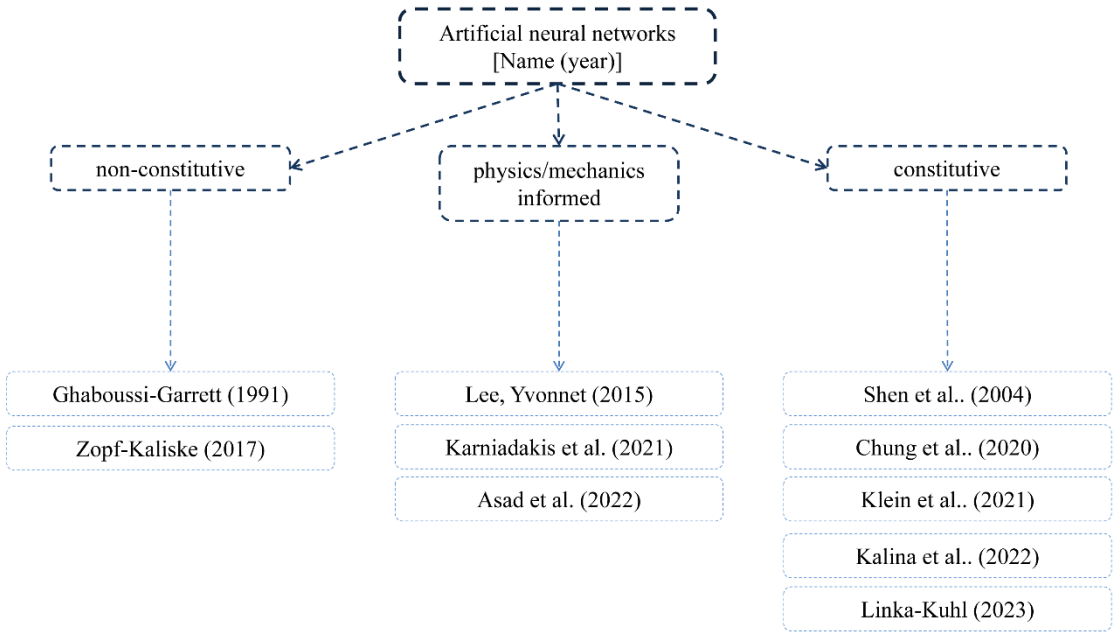

Figure 4. Different ANN (artificial neural networks) models of hyper-elastic materials.

Phenomenological models are generally based on invariants, the stretch ratio, or both. Their parameters do not bear any physical interpretation. Invariant-based phenomenological models can be further divided into models that leverage a series function, including the limitation of chain extensibility, or are based on a logarithmic function, power law, or exponential function. They were developed in the mid- and late-twentieth century and provide all analytical solutions for an isotropic single-phase

medium. The number of parameters included in their equations is small, which enables their analytical treatment of simple engineering problems. Contemporary models introduce more parameters that increase the flexibility and accuracy of calculations. The trade-off is a considerable increase in calibration and computation efforts that makes them preferable for large-scale computer simulations and not for analytical calculus.

Micromechanical models are based on the analysis of networks of cross-linked long-chain molecules. They could be subdivided into these based on a Gaussian or non-Gaussian network model, or involve a mixture of the two. Artificial neural networks could be classical and bear no mechanical constraints, or constitutive and include such constraints in the network. A comparison of various constitutive models has been provided below and notation applied in the relevant formulas is the following one: W (with various upper superscripts) denotes a function of deformation energy density, σ_{11} denotes the true Cauchy stress under uniaxial tension, μ is the shear modulus (the second Lame constant), ν is the Poisson ratio, λ_i denote principal stretches of the material (λ in uniaxial state) and J is their product. Moreover, I_1 is the first invariant of the right Cauchy-Green deformation tensor, **F** is the deformation gradient, λ_L is the first Lame constant, while C_i and D*i* as well as A_p, B_p, α_p and β_p are different material constants in the constitutive theories presented below. The Readers are encouraged to look into the given references to find a specific physical or mathematical explanation of some other parameters appearing below.

The first proposed hyper-elastic models were invariant-based, specifically the series function ones. The first theoretical approach was done by Mooney and Rivlin [53,54]. The model includes the first two invariants in their first powers:

$$W^{MR}=C_1(I_1-3)+C_2(I_2-3) \quad (1)$$

$$\sigma_{11}^{MR}=\left(2C_{1,MR}^{m}+\frac{2C_{2,MR}^{m}}{\lambda}\right)\left(\lambda^2-\frac{1}{\lambda}\right) \quad (2)$$

This model was simplified to include only the first invariant; it is widely known as the neo-Hookean model [55–57]:

$$W^{NH}= C_1(I_1-3) \quad (3)$$

$$\sigma_{11}^{NH}=2C_1\left(\lambda-\frac{1}{\lambda^2}\right) \quad (4)$$

A third, second-power term was included by Isihara [58]:

$$W^{I}= C_{10}(I_1-3) + C_{20}(I_1-3)^2+ C_{01}(I_2-3) \quad (5)$$

$$\sigma_{11}^{I}= C_{10}\left(\lambda-\frac{1}{\lambda^2}\right)+\left(\lambda^3+\frac{C_{20}}{C_{01}}-\left[1+\frac{C_{20}}{C_{01}}\right]\frac{1}{\lambda^3}\right) \quad (6)$$

Next, a third term for the first invariant was added by Yeoh [59]:

$$W^{Y}=C_1(I_1-3) + C_2(I_1-3)^2 \quad (7)$$

$$\sigma_{11}^{Y}=2(C_1 + 2C_2(I_1 - 3)+3C_3(I_1 - 3)^2)\left(\lambda-\frac{1}{\lambda^2}\right) \quad (8)$$

Carroll's model drops the conventional $(I_i\text{-}3)$ form [60] to give

$$W^{C}=\beta_1 I_1+\beta_2 I_1^4+\beta_3\sqrt{I_2} \quad (9)$$

$$\sigma_{11}^{C}=\left[2\beta_1 + 8\beta_2\left(\frac{2}{\lambda}+\lambda^2\right)^3+\beta_3\left(1+\lambda^3\right)^{-1/2}\right]\left[\lambda-\frac{1}{\lambda^2}\right] \quad (10)$$

It violates the restriction introduced by Ogden and Treolar that $U(I_1,I_2,I_3)=0$ in the reference configuration and the following modification was proposed to overcome this peculiarity:

$$W^{CM}=\beta_1(I_1-3)+\beta_2\left(I_1^4-81\right)+\beta_3\left(\sqrt{I_2}-\sqrt{3}\right) \quad (11)$$

$$\sigma_{11}^{CM}=\left[2\beta_1+8\beta_2\left(\frac{2}{\lambda}+\lambda^2\right)^3+\beta_3\left(1+\lambda^3\right)^{-1/2}\right]\left[\lambda-\frac{1}{\lambda^2}\right] \quad (12)$$

It is called a modified Carrol's model and is presented here in the incompressible form [61]. The last series function model was introduced by Zhao [62]. It adds terms with mixed invariants in different powers governed by the same constant. This concept was also used before by Bahreman and Darijani.

$$W^{Z}=C_{-1}^{1}(I_2-3)+C_1^1(I_1-3)+C_2^1(I_1^2-2I_2-3)+C_2^1(I_1^2-2I_2-3)^2 \quad (13)$$

$$\sigma_{11}^{Z}=\left[2\beta_1+8\beta_2\left(\frac{2}{\lambda}+\lambda^2\right)^3+\beta_3\left(1+\lambda^3\right)^{-1/2}\right]\left[\lambda-\frac{1}{\lambda^2}\right] \quad (14)$$

The second most common variants of phenomenological models are power, exponential, or logarithmic ones. The first one was proposed by Knowles [63]:

$$W^{K}=\frac{\mu}{2b}\left(\left(1+\frac{b(I_1-3)}{n}\right)^n-1\right) \quad (15)$$

$$\sigma_{11}^{S}=\left(\frac{1}{2}\sum_{p=1}^{N}A_p\left(\frac{I_1}{3}\right)^{\alpha_p}+\frac{1}{2}\sum_{p=1}^{N}B_p\left(\frac{I_1}{3}\right)^{\beta_p}\right)\left(\lambda-\frac{1}{\lambda^2}\right) \quad (16)$$

The next one was proposed by Swanson [64]:

$$W^{S}=\frac{3}{2}\sum_{p=1}^{N}\frac{A_p}{1+\alpha_p}\left(\frac{I_1}{3}\right)^{1+\alpha_p}+\frac{3}{2}\sum_{p=1}^{N}\frac{B_p}{1+\beta_p}\left(\frac{I_1}{3}\right)^{1+\beta_p} \quad (17)$$

$$\sigma_{11}^{S}=\left(\frac{1}{2}\sum_{p=1}^{N}A_p\left(\frac{I_1}{3}\right)^{\alpha_p}+\frac{1}{2}\sum_{p=1}^{N}B_p\left(\frac{I_1}{3}\right)^{\beta_p}\right)\left(\lambda-\frac{1}{\lambda^2}\right) \quad (18)$$

The next model was proposed by Gregory [65]:

$$W^{G}=\frac{A}{2(1-n/2)}\left(I_1-3+C^2\right)^{1-n/2}+\frac{B}{2(1-m/2)}\left(I_1-3+C^2\right)^{1-m/2} \quad (19)$$

$$\sigma_{11}^{G}=\left[A\left(I_1-3+C^2\right)^{n/2}+B\left(I_1-3+N^2\right)^{m/2}\right]\left[\lambda-\lambda^{-2}\right] \quad (20)$$

A further modification was invented recently by Hong et al. and it was called a modified Gregory model [47]:

$$W^{MG}=\frac{A}{1+\alpha}\left(I_1-3+M^2\right)^{1+\alpha}+\frac{B}{1+\beta}\left(I_1-3+N^2\right)^{1+\beta} \quad (21)$$

$$\sigma_{11}^{MG}=2\left[A\left(I_1-3+M^2\right)^{\alpha}+B\left(I_1-3+N^2\right)^{1+\beta}\right]\left[\lambda-\lambda^{-2}\right] \quad (22)$$

Another variant of a power-law-based function was put forward by Lopez-Pamies [66], where

$$W^{LP}=\sum_{r=1}^{M}\frac{3^{1-\alpha_r}}{2\alpha_r}\mu_r\left[\bar{I}_1^{\alpha_r}-3^{\alpha_r}\right] \quad (23)$$

$$\sigma_{11}^{LP}=\frac{\lambda^3-1}{2\lambda+\lambda^4}\sum_{r=1}^{M}3^{1-\alpha_r}\mu_r\left(\lambda^2+\frac{2}{\lambda}\right)^{\alpha_r} \quad (24)$$

This type of function was also proposed by Yeoh in his modified form by adding an exponential term [67]:

$$W^{Y}=C_1(I_1-3)+C_2(I_1-3)^2+C_3(I_1-3)^3+\frac{\alpha}{\beta}\left(1-e^{-\beta(I_1-3)}\right) \quad (25)$$

$$\sigma_{11}^{Y}=2(C_1+2C_2(I_1-3)+3C_3(I_1-3)^2)\left(\lambda-\frac{1}{\lambda^2}\right) \quad (26)$$

This was generalized in 2019 by Travis et al. to include arbitrary powers of all three terms. It was further called the generalized Yeoh model [68].

$$W^{GY}=C_1(I_1-3)^m+C_2(I_1-3)^p \quad (27)$$

$$\sigma_{11}^{GY}=2\left(\lambda-\frac{1}{\lambda^2}\right)mC_1(I_1-3)^{m-1}+pC_2(I_1-3)^{p-1}+qC_3(I_1-3)^{q-1} \quad (28)$$

Gent and Thomas moved away from using a power function and instead proposed a linear term combined with a relatively simple logarithmic term that allowed for a relatively easy stress formulation [69]:

$$W^{GT}= C_1(I_1-3)+C_2\ln\left[\frac{I_2}{3}\right] \quad (29)$$

$$\sigma_{11}^{GT}=\left(C_1+\frac{C_2}{\lambda}\right)\left(\lambda-\frac{1}{\lambda^2}\right) \quad (30)$$

These logarithmic or (later) exponential terms are incorporated into their energy functions to allow for a better estimation of deformation in uniaxial tension and equi-biaxial tension.

The first proposal of a combined exponential and logarithmic function was put forward by Hart-Smith [70]:

$$W^{HS}= c_{10}\int \exp(c_1[\bar{I}_1-3]^2)\,d\bar{I}_1+c_{01}\ln\left(\frac{\bar{I}_2}{3}\right) \quad (31)$$

$$\sigma_{11}^{HS}=2\left[c_{10}\exp(c_1[I_1-3]^2)+\frac{c_{01}}{\lambda I_2}\right]\left[\lambda-\frac{1}{\lambda^2}\right] \quad (32)$$

Another variant of such a combination was proposed by Alexander [71]:

$$W^{A}=c_1\int \exp(c_3[\bar{I}_1-3]^2)d\bar{I}_1+c_2\ln\left(\frac{\bar{I}_2-3+c_4}{c_4}\right)+c_3[\bar{I}_1-3] \quad (33)$$

$$\sigma_{11}^{A}=2\left(c_1\exp(c_3[I_1-3]^2)+\frac{1}{\lambda}\left[\frac{c_2c_4}{I_2-3+c_4}+c_3\right]\right)\left(\lambda-\lambda^{-2}\right) \quad (34)$$

Some other variations were put forward by Veronda and Westmann, Vito, Humphrey and Yin, and much later by Mansouri and Darijani.

Another combination of such a phenomenological model was introduced by Hoss and Marczak [72]. It consists of three terms, namely, power, exponential, and logarithmic terms:

$$W^{HM}=\frac{\alpha}{\beta}\left(1-e^{-\beta(I_1-3)}\right)+\frac{\mu}{2b}\left(\left(1+\frac{b(I_1-3)}{n}\right)^n-1\right)+C_2\ln\left(\frac{1}{3}I_2\right) \quad (35)$$

$$\sigma_{11}^{HM}=2\left(\lambda-\frac{1}{\lambda^2}\right)\left(\alpha e^{-\beta(I_1-3)}+\frac{\mu}{2}\left(1+\frac{b(I_1-3)}{n}\right)^{n-1}+\frac{1}{\lambda}\frac{C_2}{I_2}\right) \quad (36)$$

Next is the exponential-linear model [73], which instead of the summation of the logarithmic and linear terms, proposed their multiplication:

$$W^{EL}=A\left(\frac{1}{\alpha}e^{a(I_1-3)}+b(I_1-2)\left(1-\ln(I_1-2)\right)-\frac{1}{a}-b\right) \quad (37)$$

$$\sigma_{11}^{EL}=\frac{\lambda^3-1}{2\lambda+\lambda^4}\sum_{r=1}^{M}3^{1-\alpha_r}\mu_r\left(\lambda^2+\frac{2}{\lambda}\right)^{\alpha_r} \tag{38}$$

The most recent form of this type of model is the Anssari–Benam–Bucchi model [74]:

$$W^{ABB}=\mu N\left(\frac{1}{6N}(I_1-3)-\ln\left(\frac{I_1-3N}{3-3N}\right)\right) \tag{39}$$

$$\sigma_{11}^{ABB}=2\mu\frac{9N-\left(\lambda^2+2\lambda^{-1}\right)}{3N-\left(\lambda^2+2\lambda^{-1}\right)}\left(\lambda^2-\frac{1}{\lambda}\right) \tag{40}$$

Another type of phenomenological model limits chain extensibility. This type introduces a limit for the stretch ratio for the macromolecular chain of rubber I_m and provides other parameters for small strains. The first one was introduced by Warner [75]:

$$W^{W}=-\frac{\mu I_m}{2}ln\left(1-\frac{I_1-3}{I_m-3}\right) \tag{41}$$

$$\sigma_{11}^{W}=\left(\frac{1}{2}\sum_{p=1}^{N}A_p\left(\frac{I_1}{3}\right)^{\alpha_p}+\frac{1}{2}\sum_{p=1}^{N}B_p\left(\frac{I_1}{3}\right)^{\beta_p}\right)\left(\lambda-\frac{1}{\lambda^2}\right) \tag{42}$$

A further proposal with a much more elaborate logarithmic term was made by van der Waals [76]. It includes the limit stretch λ_m:

$$W^{VW}=-\mu[\lambda_m-3][\ln(1-\theta)+\theta]-\frac{2}{3}\left(\frac{\tilde{I}-3}{2}\right)^{\frac{3}{2}},\ \theta=\sqrt{\frac{\hat{I}-3}{\lambda_m^2-3}},\hat{I}=\beta I_1+(1-\beta)I_2 \tag{43}$$

$$\sigma_{11}^{VW}=\left(\left[\beta+\lambda^{-1}-\beta\lambda^{-1}\right]\left[\frac{\mu}{1-\eta}-a\mu\left(\frac{\tilde{I}-3}{2}\right)^{1/2}\right]\right)\left(\lambda-\lambda^{-2}\right) \tag{44}$$

A small difference in the quotient was then proposed by Gent [77]. It allowed for better accuracy for small stretches:

$$W^{G}=-\frac{\mu J_m}{2}\ln\left[1-\frac{I_1-3}{J_m}\right] \tag{45}$$

$$\sigma_{11}^{G}=\left(\frac{\mu J_m}{J_m-I_1+3}\right)\left(\lambda-\frac{1}{\lambda^2}\right),\ J_m=I_m-3,\ I_1=\lambda^2+\frac{2}{\lambda} \tag{46}$$

In the early 2000s, Pucci and Saccomandi [78] proposed a model with two logarithmic terms:

$$W^{PS}=-J_m\frac{\mu}{2}\ln\left(1-\frac{\bar{I_1}-3}{J_m}\right)+c_2\ln\left(\frac{\bar{I_2}}{3}\right) \tag{47}$$

$$\sigma_{11}^{PS}=\left(\frac{J_m\mu}{J_m-I_1+3}+\frac{2c_2}{\lambda I_2}\right)\left(\lambda-\lambda^{-2}\right) \tag{48}$$

The last variant of this kind of phenomenological model was put forward by Horgan and Murphy [79]:

$$W^{HM}=\frac{2\mu(I_m-3)}{c^2}\ln\left(1-\frac{\lambda_1^c+\lambda_2^c+\lambda_3^c}{I_m-3}\right) \tag{49}$$

$$\sigma_{11}^{HS}=\left(\frac{J_m\mu}{J_m-I_1+3}+\frac{2c_2}{\lambda I_2}\right)\left(\lambda-\lambda^{-2}\right) \tag{50}$$

Phenomenological models based on the stretch ratio are simple, yet could be used for large strain ratios, especially the famous Ogden variant. The first one was proposed by Valanis and Landel [80]:

$$W^{VL}=2\mu\sum_{i=1}^{3}\left(\lambda_i\ln(\lambda_i-1)\right) \tag{51}$$

$$\sigma_{11}^{VL}=I_3^{-1/2}\lambda_i\frac{\partial W}{\partial\lambda_i} \tag{52}$$

Its compressible form and additional proofs and its experimental validation is also provided in [81]. Further proposals were prepared by Ogden [14]:

$$W^{O}=\sum_{r=1}^{M}\frac{\mu_r}{\alpha_r}\left[\lambda_1^{\alpha_r}+\lambda_2^{\alpha_r}+\lambda_3^{\alpha_r}-3\right] \tag{53}$$

$$\sigma_{11}^{O}=2\frac{\mu_r}{\alpha_r}\lambda^{\alpha_r}-\frac{1}{\sqrt{\lambda}}^{\alpha_r} \tag{54}$$

- Shariff [13]:

$$W^{S}=\omega(\lambda_1)+\omega(\lambda_2)+\omega(\lambda_3)=E\sum_{j=0}^{n}\alpha_j\varphi_j(\lambda_i) \tag{55}$$

$$\sigma_{11}^{S}=\frac{E}{\lambda}\begin{bmatrix}\ln\lambda+\alpha_1\vartheta_1+\alpha_2\vartheta_1\\+\alpha_3\left[\frac{\vartheta_2}{\lambda^{3.6}}-\frac{\vartheta_3}{\lambda^{-1.8}}\right]\\+\alpha_4[\vartheta_2-\vartheta_3]\end{bmatrix} \tag{56}$$

$$\vartheta_1=\left[e^{1-\lambda}-e^{1-\lambda^{\frac{1}{2}}}+\lambda-\lambda^{\frac{1}{2}}\right],\ \vartheta_2=(\lambda-1)^3,\vartheta_3=\left(\lambda^{\frac{1}{2}}-1\right)^3$$

- Attard and Hunt [25]:

$$W^{AH}=\sum_{r=1}^{M}\frac{A_r}{2r}\mathrm{tr}\left(\bar{\mathbf{C}}^{\mathbf{r}}-\mathbf{I}\right)+\frac{B_r}{2r}\mathrm{tr}\left(\bar{\mathbf{C}}^{\mathbf{r}}-\mathbf{I}\right),\ \mathrm{tr}\left(\bar{\mathbf{C}}^{\mathbf{r}}-\mathbf{I}\right)=\left[\bar{\lambda}_1^{2r}+\bar{\lambda}_2^{2r}+\bar{\lambda}_3^{2r}-3\right] \tag{57}$$

$$\sigma_{11}^{AH}=\sum_{r=1}^{M}A_r\left[\lambda^{2r-1}-\lambda^{-r-1}\right]+B_r\left[\lambda^{r-1}-\lambda^{-2r-1}\right] \tag{58}$$

- and Arman and Narooei [82]:

$$W^{AN}=\sum_{p=1}^{N}A_p\left(exp\left[m_p\left(\lambda_1^{\alpha_p}+\lambda_2^{\alpha_p}+\lambda_3^{\alpha_p}-3\right)\right]-1\right)+\sum_{q=1}^{N}B_q\left(exp\left[n_q\left(\lambda_1^{-\beta_q}+\lambda_2^{-\beta_q}+\lambda_3^{-\beta_q}-3\right)\right]-1\right) \tag{59}$$

$$\sigma_{11}^{AN}=\frac{E}{\lambda}\begin{bmatrix}\ln\lambda+\alpha_1\vartheta_1+\alpha_2\vartheta_1\\+\alpha_3\left[\frac{\vartheta_2}{\lambda^{3.6}}-\frac{\vartheta_3}{\lambda^{-1.8}}\right]\\+\alpha_4[\vartheta_2-\vartheta_3]\end{bmatrix} \tag{60}$$

Mixed phenomenological models use invariants and stretch ratios that can capture small and high strains well. They emerged in the early 2000s. Some examples are the continuum hybrid model [83]:

$$W^{CH}=K_1(I_1-3)+K_2\ln\frac{I_2}{3}+\frac{\mu}{\alpha}(\lambda_1^{\alpha}+\lambda_2^{\alpha}+\lambda_3^{\alpha}-3) \tag{61}$$

$$\sigma_{11}^{CH}=I_3^{-1/2}\lambda_i\frac{\partial U}{\partial\lambda_i} \tag{62}$$

and the WFB model [84]:

$$W^{WFB}=\int_1^{L_f}\left(F(\lambda_1)A(\lambda_1e^{-BI_1})+C\left(\lambda_1I_1^{D}\right)\right)\left(\lambda_1^2-\frac{1}{\lambda_1}\right)d\lambda_1 \tag{63}$$

$$\sigma_{11}^{WFB}=I_3^{-1/2}\lambda_i\frac{\partial U}{\partial\lambda_i} \tag{64}$$

Micromechanical network models aim to determine the microstructural mechanisms of the material that relate to their mechanical properties. They can be categorized by the presence of a Gaussian character in the chain network. Gaussian chain network models characterize small and moderate stretches well but are not as accurate for large ones with hardening. The first Gaussian model was proposed by Treloar [85]:

$$W^G=\frac{1}{2}NkT\left(\lambda_1^2+\lambda_2^2+\lambda_3^2-3\right) \tag{65}$$

$$\sigma_{11}^G=I_3^{-1/2}\lambda_i\frac{\partial U}{\partial\lambda_i} \tag{66}$$

Some other variants include the slip-link model [86]:

$$W^{SL}=\frac{1}{2}G_e\sum_{i=1}^{3}\left(\frac{(1+\eta)(1-\alpha^2)\lambda_i^2}{(1+\eta\lambda_i^2)(1-\alpha^2\sum_{i=1}^{3}\lambda_i^2)}+ln\left(1+\eta\sum_{i=1}^{3}\lambda_i^2\right)\right) \tag{67}$$

$$\sigma_{11}^{SL}=\mu_c\left(\lambda-\lambda^{-2}\right)+\frac{2\mu_e}{\beta}\left(\lambda^{\frac{\beta}{2}-1}-\lambda^{-\beta-1}\right) \tag{68}$$

and also the tube [43] model. The tube model potential consists of two parts that characterize chain cross-linkings $W^{T,c}$ and chain entanglements $W^{T,e}$ such that

$$W^T=W^{T,c}+W^{T,e}=\sum_{i=1}^{3}\frac{\mu_c}{2}\left(\overline{\lambda}_i^2-1\right)+\frac{2\mu_e}{\beta^2}\left(\overline{\lambda}_i^{-\beta}-1\right) \tag{69}$$

$$\sigma_{11}^T=\mu_c\left(\lambda-\lambda^{-2}\right)+\frac{2\mu_e}{\beta}\left(\lambda^{\frac{\beta}{2}-1}-\lambda^{-\beta-1}\right) \tag{70}$$

The most recent Gaussian-type model is a nonaffine tube model [87] characterized as

$$W^{NT}=W^{ph}+W^{ent}=G_c\sum_{i=1}^{3}\frac{\lambda_i^2}{2}+G_e\sum_{i=1}^{3}\left(\lambda_i+\frac{1}{\lambda_i}\right) \tag{71}$$

$$\sigma_{11}^{NT}=\mu_c\left(\lambda-\lambda^{-2}\right)+\frac{2\mu_e}{\beta}\left(\lambda^{\frac{\beta}{2}-1}-\lambda^{-\beta-1}\right) \tag{72}$$

Non-Gaussian chain network models apply the mechanical property of a non-Gaussian single chain to the molecular chains of the rubber network. The first three-chain model assumed a distribution of molecular chains along principal directions and was efficient only for small stretches. This limitation was overcome by Arruda and Boyce by introducing limited chain extensibility. Furthermore, a more general distribution of molecular chains was allowed in further theories that also introduced chain entanglement and cross-linking.

The three-chain model is defined in the following manner [88]:

$$W^{3C}=\frac{\mu N}{3}\sum_{i=1}^{3}\left(\overline{\gamma}_i\overline{\lambda}_{r,i}+\ln\left(\frac{\overline{\gamma}_i}{\sinh\overline{\gamma}_i}\right)\right) \tag{73}$$

$$\sigma_{11}^{3C}=\frac{\mu}{3\lambda}\left(\lambda^2\left[\frac{3N-\lambda^2}{N-\lambda^2}\right]-\frac{1}{\lambda}\left[\frac{3N-\lambda^{-1}}{N-\lambda^{-1}}\right]\right) \tag{74}$$

The well-known and frequently used Arruda–Boyce model is presented next [89]:

$$W^{AB}=C_1\left(\begin{array}{c}\left(\frac{1}{2}I_1-3\right)+\frac{1}{20(\lambda_A)^2}+\frac{1}{1050(\lambda_A)^4}\left(I_1^3-27\right)+\\ \frac{19}{7000(\lambda_A)^6}\left(I_1^4-81\right)+\frac{519}{673750(\lambda_A)^8}\left(I_1^5-243\right)\end{array}\right)=C_1\sum_{i=1}^{5}\alpha_i\widehat{\beta}^{i-1}\left(I_1^i-3^i\right) \quad (75)$$

$$\sigma_{11}^{AB}=2C_1\left(\lambda-\frac{1}{\lambda^2}\right)\left(\begin{array}{c}\frac{1}{2}+\frac{2}{20(\lambda_A)^2}(I_1-9)+\frac{3}{1050(\lambda_A)^4}\left(I_1^2-27\right)+\\ \frac{4\cdot19}{7000(\lambda_A)^6}\left(I_1^3-81\right)+\frac{5\cdot519}{673750(\lambda_A)^8}\left(I_1^4-243\right)\end{array}\right) \quad (76)$$

- The eight-chain model is as follows [90]:

$$W^{8C}=\frac{\mu N}{3}\left(\overline{\gamma}\overline{\lambda}_r+\ln\left(\frac{\overline{\gamma}}{\sinh\overline{\gamma}_i}\right)\right) \quad (77)$$

$$\sigma_{11}^{8C}=\frac{\mu}{3}\left(\left[\frac{3N-\lambda_{cu}^2}{N-\lambda_{cu}^2}\right]\right)\left(\lambda-\lambda^{-2}\right),\ \lambda_{cu}=\sqrt{\frac{1}{3}\left(\lambda^2+\frac{2}{\lambda}\right)} \quad (78)$$

A systematical consideration of the affine, three-chain, eight-chain, and micro-sphere models is provided in [91].

The Flory–Erman approach, which is an extension of the nonaffine-tube model and consists of the phantom energy $W^{FE,pe}$ function and micromechanics of chain molecules $W^{FE,ce}$, is provided in the following way [92]:

$$\begin{array}{c}W^{FE}=W^{FE,pe}+W^{FE,ce}=\sum_{i=1}^{3}\frac{\mu}{2}\left(\left[1-\frac{1}{\phi}\right]\left[\overline{\lambda}_i^2-1\right]+[B_i+D_i-\ln(B_i+1)-\ln(D_i+1)]\right)\\ \xi=\left[1-\frac{1}{\phi}\right]n,\ \mu=nK\theta,\ B_i=\kappa^2\left(\overline{\lambda}_i^2-1\right)\left(\overline{\lambda}_i^2+\kappa\right)^{-2},\ D_i=\overline{\lambda}_i^2\kappa^{-1}B_i\end{array} \quad (79)$$

$$\sigma_{11}^{FE}=\mu\left(1-\frac{2}{\phi}\right)\left(\lambda-\lambda^{-2}\right)+\frac{\partial U_{FE,ce}^{m}}{\partial\lambda_i} \quad (80)$$

The Gaussian nature of the phantom part of this model causes a deviation at high strains. This is overcome in its modified version proposed by Boyce and Arruda. It replaces the neo-Hookean part with an eight-chain model such that

$$W^{FE,m}=W^{8C}+W^{FE,ce}=\mu N\left(\overline{\gamma}\overline{\lambda}_r+\ln\left(\frac{\overline{\gamma}}{\sinh\overline{\gamma}_i}\right)\right)+\sum_{i=1}^{3}\frac{\mu}{2}([B_i+D_i-\ln(B_i+1)-\ln(D_i+1)]) \quad (81)$$

$$\sigma_{11}^{FE,m}=\sigma_{11}^{8C}+\frac{\partial W^{FE,ce}}{\partial\lambda_i} \quad (82)$$

In its simplified version, the micro-sphere model [93] is given as

$$W^{MS}=\mu\left(\lambda_r L^{-1}(\lambda_r)+\ln\left(\frac{\gamma}{\sinh(\gamma)}\right)\right) \quad (83)$$

$$\sigma_{11}^{MS}=\mu_c\left(\lambda-\lambda^{-2}\right)+\frac{2\mu_e}{\beta}\left(\lambda^{\frac{\beta}{2}-1}-\lambda^{-\beta-1}\right) \quad (84)$$

One of the modern formulations of a hyper-elastic material is the extended tube model [94], which includes five parameters. It focuses on the molecular–statistical approach for polymer networks and it is based on the following formulae:

$$W^{ET}=\frac{\mu_c}{2}\left(\frac{(1-\delta^2)(\bar{I}_1-3)}{1-\delta^2(\bar{I}_1-3)}+\ln\left(1-\delta^2(\bar{I}_1-3)\right)\right)+\sum_{i=1}^{3}\frac{2\mu_e}{\beta^2}\left(\bar{\lambda}_i^{\beta}-1\right) \quad (85)$$

$$\sigma_{11}^{ET}=\mu_c\left(\lambda-\lambda^{-2}\right)\left(\frac{1-\delta^2}{\left(1-\delta^2(I_1-3)\right)^2}-\frac{\delta^2}{1-\delta^2(I_1-3)}\right)+\frac{2\mu_e}{\beta}\left(\lambda^{\frac{\beta}{2}-1}-\lambda^{-\beta-1}\right) \quad (86)$$

- Network averaging tube [95]:

$$W^{NA}=\mu_c\kappa n\ln\left(\frac{\sin\left(\frac{\Pi}{\sqrt{n}}\right)\left(\frac{I_1}{3}\right)^{q/2}}{\sin\left(\frac{\Pi}{\sqrt{n}}\left(\frac{I_1}{3}\right)^{q/2}\right)}\right) \quad (87)$$

$$\sigma_{11}^{NA}=\frac{\mu}{3}\left(\left[\frac{3N-\lambda_{cu}^2}{N-\lambda_{cu}^2}\right]\right)\left(\lambda-\lambda^{-2}\right) \quad (88)$$

- SpT [96]:

$$W^{SpT}=G_cN\ln\left(\frac{3N+\frac{1}{2}I_1}{3N-I_1}\right)+G_e\sum_i\lambda_i \quad (89)$$

$$\sigma_{11}^{SpT}=\frac{\mu}{3}\left(\left[\frac{3N-\lambda_{cu}^2}{N-\lambda_{cu}^2}\right]\right)\left(\lambda-\lambda^{-2}\right) \quad (90)$$

- Wu-Giessen or full-network [97]:

$$W^{FN}=W^{3C}(1-\varrho)+\varrho W^{8C} \quad (91)$$

$$\sigma_{11}^{FN}=\sigma_{11}^{3C}(1-\varrho)+\varrho\sigma_{11}^{8C} \quad (92)$$

- Lim [98]:

$$W^{L}=W^{G}(1-f)+fW^{8C} \quad (93)$$

$$\sigma_{11}^{S}=\left(\frac{1}{2}\sum_{p=1}^{N}A_p\left(\frac{I_1}{3}\right)^{\alpha_p}+\frac{1}{2}\sum_{p=1}^{N}B_p\left(\frac{I_1}{3}\right)^{\beta_p}\right)\left(\lambda-\frac{1}{\lambda^2}\right) \quad (94)$$

- Bechir and Chavalier [99]:

$$W^{WG}=\frac{3}{2}\sum_{p=1}^{N}\frac{A_p}{1+\alpha_p}\left(\frac{I_1}{3}\right)^{1+\alpha_p}+\frac{3}{2}\sum_{p=1}^{N}\frac{B_p}{1+\beta_p}\left(\frac{I_1}{3}\right)^{1+\beta_p} \quad (95)$$

$$\sigma_{11}^{S}=\left(\frac{1}{2}\sum_{p=1}^{N}A_p\left(\frac{I_1}{3}\right)^{\alpha_p}+\frac{1}{2}\sum_{p=1}^{N}B_p\left(\frac{I_1}{3}\right)^{\beta_p}\right)\left(\lambda-\frac{1}{\lambda^2}\right) \quad (96)$$

Only recently have some efforts been made to define the hyper-elastic behavior of multi-phase materials. This was because of the high complexity of numerical simulations and the unavailability of analytical solutions. These problems were overcome by a rapid increase in computational resources, allowing for an iterative solution. Some examples of contemporary studies include [100–108], as well as [109] for the visco-elastic regime. Demand for advanced hyper-elastic models is stimulated by the biotechnological industry, where the mechanics of biological tissue [110] and its interaction with artificial appliances were studied [21]. They are also required in aerial, textile, and automotive industries, and are used, for example, in tires or various shock absorbers. It needs to be mentioned that Poisson ratio close to the value of 0.5 for rubber-like materials may break

the FEM solution incremental processes (in both deterministic and probabilistic context) due to the negative diagonal components within the stiffness matrix or a lack of numerical convergence.

Unlike in linear small strain elasticity, all the models provide their own set of assumptions that were prescribed during the derivation process and are not necessarily easily interchangeable with others. This introduces challenges in the description of their stochastic nature because the material parameters are not a good choice for overall stochastic unknowns. Such a choice would bind the analysis to a specific model, which is highly undesirable. Instead, some more generic parameters or variables should be preferred, for example, a defects volume fraction, which is unique for all models; random (effective) material coefficients should instead be derived from other random sources.

Stochastic or probabilistic studies are quite well documented in the reversible elastic regime of composites [111,112]. This is not true for the inelastic regime. One of the main reasons is the abovementioned lack of generality of various laws and the complexity of their numerical solution already given in the deterministic case. The stochastic hyper-elasticity or visco-elasticity of composites is considered only in a limited number of studies; some examples include [113–116]. Much attention was focused on a certain hyper-elasticity potential, for example, the Ogden [117–119], neo-Hookean [66,120], or van der Waals models [105]; some of these also compare the results of several potentials, as in [121], or propose a specific solution technique [122]. However, there is a lack of studies concerning the composites that include interface defects in the nonlinear regime. This is especially true for a joint deterministic and stochastic analysis coupled with the verification of multiple hyper-elastic potentials. Unlike the majority of the stochastic considerations, these analyses are additionally based on the set of laboratory tests performed especially for the computational part, for which the numerical response of the matrix is fitted with the use of the least squares method. The proposed approach specifically tackles the problem of the lack of generality of hyper-elastic laws via the introduction of a probabilistic homogenization algorithm for probabilistic homogenization. It enables the computation of random effective material parameters for an arbitrary linear hyper-elastic potential with a specified source of the input uncertainty.

Please note that the engineering stress σ_i for the above models can be obtained for all the principal directions i using the following formulae:

$$\sigma_i = \frac{\partial W}{\partial I_1}\frac{\partial I_1}{\partial \lambda_i} - \frac{\partial W}{\partial I_2}\frac{\partial I_2}{\partial \lambda_i} - \frac{1}{\lambda_i}p \tag{97}$$

and thus, for uniaxial tension, $\sigma_1^{UT}=2\left(\frac{\partial W}{\partial I_1}+\frac{1}{\lambda}\frac{\partial W}{\partial I_2}\right)\left(\lambda-\frac{1}{\lambda^2}\right)$ and $\sigma_2^{UT}=\sigma_3^{UT}=0$; for pure shear, $\sigma_1^{PS}=2\left(\frac{\partial W}{\partial I_1}+\frac{\partial W}{\partial I_2}\right)\left(\lambda-\frac{1}{\lambda^3}\right)$, $\sigma_2^{PS}=2\left(\frac{\partial W}{\partial I_1}+\lambda^2\frac{\partial W}{\partial I_2}\right)\left(\lambda-\frac{1}{\lambda^2}\right)$, and $\sigma_3^{PS}=0$; and for equi-biaxial tension, $\sigma_1^{BT}=2\left(\frac{\partial W}{\partial I_1}+\frac{1}{\lambda}\frac{\partial W}{\partial I_2}\right)\left(\lambda-\frac{1}{\lambda^5}\right)$ and $\sigma_3^{BT}=0$.

Artificial neural networks emerged in constitutive model determination 30 years ago [123]. Instead of first selecting its closed form and then the tuning parameters, they propose a family of artificial neural networks and then learn its weight and parameters; they may be physical, phenomenological, or mixed. Until recently, classical neural networks remained a black box in terms of the morphology of parameters and partially or totally disregarded the kinematic, thermodynamic, and physical constraints. They also bypassed constitutive modeling altogether. This raised well-posed concerns for their formulation. These were covered recently via the direct inclusion of the physical and mechanical constraints into the neural network [124–126].

A very interesting innovation in this regard constitutes artificial neural networks. They take an a priori closed set of constitutive models whose distribution in the final formula is defined during the learning process [127,128]; such a formulation overcomes the above concerns. Such a trained network includes a sum-of-weighted closed-form models for each loading scheme. Thus, it is not strictly a new model in itself but is rather

a novel mixture of already created ones; its successful utilization requires prior knowledge of classical models and cannot work without them.

3. Probabilistic Methods

The structural behavior of materials and structures in civil and mechanical engineering design is defined by models with specific assumptions. Traditionally they have a certain set of parameters to fit them to the response of the material in well-known tests. These parameters are always exposed to some scatter, which comes from various sources of randomness, such as the morphology of the material, tolerances in manufacturing and measurements, accuracy of conversions, or other unknown origins that are impossible to quantify during measurement.

Probabilistic analysis is an approach that tackles this problem directly by augmenting deterministic mathematical models with random parameters or variables that represent sources of uncertainty. It allows for a much more precise estimation of the behavior of the analyzed system. In addition to the mean, characteristic, or design values obtained in most engineering calculations, it also outputs the expected value, coefficient of variation, and other specific information about the uncertainty of the results. It further allows us to directly compute and optimize the structural safety margin in certain load conditions. This margin may be represented, for example, as a reliability index or probability of survivability. Probabilistic analysis may be applied in almost all (and not only) structural analyses at various levels of design, i.e., the level of material, structural element, or even the level of the entire structure; recent examples include heat transfer [129,130], fatigue [131,132], stiffness [133], failure [134–136], or system response under uncertainty [137].

The probabilistic approach encompasses all the methods based on probability calculus, leading to the calculation of the material or structural response with input uncertainties. This response is commonly represented as random moments or characteristics, such as the expected value, coefficient of variation, skewness, or kurtosis [138]. The most precise representation of statistical distribution is the probability density function (PDF), but it is also the most demanding in terms of computational resources. This is why in most cases, probabilistic characteristics are preferable, as in the study of hyper-elastic materials. The most widespread methods that allow for probabilistic design are direct derivation methods, simulation methods, spectral methods, and perturbation methods.

Direct derivation methods [14,138] use integral calculus to derive random characteristics of the response with a known PDF of the input random variables. In its classical form, this approach uses a direct relation between the structural response and the random parameter; it is commonly called an analytical method (AM). In many cases, such a relation is not known, cannot be derived analytically, or a symbolic solution for the known relation simply does not exist. An approximation of this relation is obtained with various numerical techniques that are commonly called a response function or a response surface. Such an approach is called a semi-analytical method (SAM) [138,139] and is applied in the study of hyper-elastic materials; alternatively, some approximate integration may be employed.

Computer simulation methods [140–145] substitute integration with a finite number of deterministic realizations, which are then subjected to statistical estimation. Realizations are made with sets of parameters obtained from random or pseudo-random generation according to their predefined PDFs; these are all referred to as Monte Carlo simulation (MCS) methods [140,146,147]. They have some advantages, i.e., ease of implementation and avoidance of integration, but they all also have important disadvantages. The major drawback of this approach is the vast number of realizations required to reach a satisfactory convergence result, which is guaranteed only with their infinite number [140,148]. This problem is partially covered in more modern approaches, such as importance sampling [149], stratified sampling [150], or Latin hypercube sampling [151] techniques; all of these approaches attempt to lower the required sampling number.

A second disadvantage is poor scaling for an increasing number of unknowns. The last and deciding disadvantage is that the inherent discrete character of the MCS disables the retrieval of continuous probabilistic characteristics or measures of reliability.

The spectral method [130,152–154] describes the Gaussian random field with the use of the Karhunen–Loève expansion. The structural response is emulated by expansion into polynomial chaos [155], but the biggest problem of this methodology is the number of terms in the expansion series necessary to achieve satisfactory accuracy [156]. Because of this, the result may be inadequate and quite far from the exact solution, especially when a second-order polynomial is used (which is commonly done). For this expansion to obtain satisfactory accuracy, a high number of elements may oftentimes be required. An additional problem is connected to the Karhunen–Loève expansion itself, which does not have a solution for certain problems [157,158], with an especially important example being a reliable calculation of higher-order probabilistic characteristics [159].

Perturbation methods [138,159,160] describe the structural response as spread around its mean value with a given small perturbation. They expand the response function into a Taylor series around the expected values of random variables. The order of this method depends on the number of terms in the applied expansion, namely, one term in the first order, two terms in the second order, etc. One of its issues is the convergence of the Taylor series, which is not always guaranteed. This problem is even more complex when the response function is not known and must be approximated, which is the case for the study of hyper-elastic materials. The response function is selected from a set of polynomial functions, where the theoretical convergence of specific Taylor series can be mathematically proven. The major advantages of this method are swift execution, relative ease of implementation, and continuous character of the results. It also substitutes integrals with derivatives and overcomes the problem of the lack of an analytical solution. The biggest drawback is the probabilistic convergence for certain types of functions and the requirement of a higher order expansion to reach high accuracy for input random variables with a high coefficient of variation. A relation between the result and the input random variable is usually unknown before the probabilistic analysis. Its analytical derivation is available only for relatively simple, well-known problems. In other cases, this relation is sought with the use of numerical methods, such as the finite element method, boundary element method, and finite difference method; joining their output with probabilistic analysis results in the stochastic finite element method (SFEM) [153,161–164], stochastic boundary element method (SBEM) [165,166], and stochastic finite difference method (SFDM) [138,167]. Such a fusion creates a powerful tool for probabilistic design and stochastic computations but it does not provide a new probabilistic method itself. This is because of the convenience of solving the homogenization problem and the availability of software for FEM computations; readers looking for a comprehensive introduction to the finite element method may refer to [168].

4. Interphase and Interface Defects

An interphase is an additional phase of the composite formed during its manufacturing process or exploitation. It is introduced (artificially in modeling or during manufacturing) in between two phases of a composite, commonly between the matrix and the filler (reinforcement). Its mechanical [169], thermal, electrical, thermo-mechanical [170], and physical characteristics differ from the ones of the two surrounding phases. Its volume is much lower than the other phases, yet it highly influences the behavior of an entire composite. This is because the interphase effectively encapsulates the filler and prevents a direct interaction in between the composite constituents. As documented, an interphase significantly affects the effective material properties of multiple isotropic, cubic, and anisotropic composites in a deterministic [171–175] and also stochastic context [8,11,176,177]. It either decreases them in the existence of defects [178] or increases when the two phases are chemically bound [179–182]. Its influence is so high that considerable

research attention has been put toward its tuning and tweaking to improve key properties of composites or adjust their performance for special purposes [183,184].

An interphase is extremely difficult to localize and further analyze in laboratory tests. This is because its thickness is very small (in the order of micrometers) and its characteristics differ for each particle or fiber in the same sample of the composite. Despite the existence of multiple surface agents applied in the phases, the interphase around each filler particle or fiber has unique thermo-electro-mechanical conditions in which it forms; this effectively causes its geometry, thickness, and properties to be random (see [185]).

Interface defects encompass all the inclusions, voids, discontinuities, and inaccuracies that exist in the transition of the two phases in a composite. They reflect frequent manufacturing imperfections, for instance, following significant residual thermal stresses, and can be treated during a numerical simulation as geometrical imperfections in composite materials [186]. Their occurrence greatly affects the response and properties of the composite despite its extremely small volume, which is a fraction of the volume of the interphase. Interface defects were shown to be crucial for many properties of a composite, including its durability [187], reliability [188], thermal conductivity [189], and even failure [180,190–192]. The defects and inclusions also cause a high microscopic stress concentration [193]. Some studies were devoted to the defects only [194].

An interphase with interface defects forms an imperfect interface. Its usage in the realistic prediction of composites' behavior dates back many years [195–199]. The analysis of composites with imperfect interfaces is performed primarily with the use of three techniques: (1) insertion of the interphase in between the main composite constituents [200–204], (2) usage of special contact finite elements [205,206], and (3) an application of a system of the springs [207] that may also be supplemented with dumpers. Very interesting strategies belonging to the first group are based upon a geometrical idealization of such defects, e.g., with the use of semi-circular or semi-spherical shapes, which follows the well-known cavitation phenomenon for a variety of matrices [190,208].

5. Multiscale Models and Numerical Simulation

Multiscale analysis represents some trends in current numerical modeling in which the given heterogeneous system is described simultaneously by multiple models at different scales of resolution. Models at each scale may originate from physical laws of different natures, for example, continuum mechanics at the macroscale [209] and molecular dynamics at the atomistic scale. They are required because certain phenomena visible at one scale cannot be described accurately without supplementary information from a different scale from which they originate. Some examples include (1) brittle failure of the reinforced concrete beam, which is caused by micro-cracks in concrete microstructure in between the cement and grains; (2) plastic elongation of steel caused by a slip between its grains; or (3) macroscopic properties of composites affected by microstructural defects. Alternatively, they are used because purely macroscale models are not accurate enough, while lower-scale models offer too much information or require too high computational power to be executed. The multiscale approach aims at achieving a compromise between accuracy and efficiency and frequently provides solutions to problems that are otherwise unsolvable in a reasonable period. The multiscale analysis comprises three major components: multiscale models, multiscale analysis tools, and multiscale algorithms. Multiscale algorithms involve using multiscale analysis tools to bridge the scales and connect different multiscale models at different levels.

The most used scales depend mainly upon the dimensions and are the following: macroscale, mesoscale (level of microstructure), atomistic scale, and electronic scale. Interestingly, each of these scales falls into a different discipline, for example, the macroscale falls into civil and mechanical engineering, the mesoscale falls into materials science, and the electronic scale falls into physics. Thus, multiscale design frequently requires bridging different disciplines to be solved. The connection between the models is either ensured analytically or numerically [210–212] and bridging between different

scales is either done sequentially or concurrently. In the sequential approach, certain characteristics used in macroscopic models are precomputed. Usually, only a limited number of the parameters (or variables) is passed to a different scale, but in some sparse representations, even as many as six variables can be passed effectively [213,214]. In the concurrent alternative, the macroscale model variables are computed on the fly during simulation. Its major advantage is that a much smaller domain of macroscopic variables must be computed on a different scale. On the other hand, the complexity of numerical algorithm solving macroscale increases. Concurrent methods are not especially well suited to problems in which parameters are passed to the FEM-based code, where each element would potentially require a separate set of parameters.

Traditional structural analysis preferred in civil engineering does not involve a multiscale approach because it tends to limit calculations to a linear range of material deformation, where simple empirical constitutive laws are sufficient. The additional margin of a nonlinear structural response is frequently used as a safety margin. A good example is the design of structures made from constructional steel, for which the engineering codes, such as Eurocodes, prefer the usage of linear elastic models. Calculations become much more involved (even for steel) when localized phenomena, such as strain localization [215] or crystal plasticity [216], must be taken into consideration. For these phenomena, a macroscale model must be supplemented or interchanged with a macroscopic structure. Macroscopic stress in the FEM crash test is calculated with supplementary information from the mesoscale (scale of crystals and phases), as well as lower scales, where defects originate. Unlike in statics, in structural dynamics, a scale is not only defined for space, but also for time. The smaller the scale, the lower the dimensions and the smaller the timespan. In multiscale design, information may be passed from a higher scale into a lower scale (top-down method) or from a lower to a higher scale (bottom-up method).

The process of crossing a certain scale is called scale-bridging; an example of top-down bridging is passing boundary conditions for each element of the FEM analysis into a mesoscale model, while a bottom-up bridging example involves intra-grain bonding conditions coming from the atomistic scale. A multiscale approach is already used, albeit indirectly, at the structural design level for reinforced concrete. Verification of the ultimate limit state for this composite already requires some supplementary information apart from the scale of the structural element. Specifically, precise information on steel rebar positioning is required even when all the macroscopic properties of concrete and steel are already known. These properties already depend on information coming from four lower scales, i.e., C-S-H, cement paste, mortar, and concrete mesoscale scales [217].

There exist multiple methods and algorithms that allow for solving multiscale problems. They focus on algebraic, numerical, or hybrid solutions and are usually aimed at certain problem domains. Their comprehensive review is available in [218]. Some examples include the multi-grid methods aimed at solving a large system of algebraic equations [219] with some alteration in the equation-free method [220] and a heterogeneous multiscale method where a preconceived macroscale model with missing components is assembled and missing data is found with the use of microscale models or matched asymptotics approach [221–223]. Some other methods include averaging and tolerance-averaging methods [224,225], hydrodynamic limit methods [226], the Mori–Zwanzig formalism [227], renormalization group methods [228], variational methods [229], and homogenization methods [230–236]**.** The multiscale approach is very frequently used for the determination of the macroscopic (or effective) properties of composites, also in the stochastic context [237,238]. Some introduction to their theory is available, for example, in [239,240]. The homogenization method is often chosen because of its relatively easy application in FEM systems.

6. Homogenization Method and Effective Medium Response

The homogenization method is frequently referred to as a process of the replacement of an equation with a highly oscillatory coefficient with one that has a homogenous coefficient. Initially used in studying partial differential equations (PDEs) [230,241], this concept was found to be efficient at solving a problem of the non-homogenous microstructure of continua, such as composites. This is because the macroscale boundary conditions, such as forcings, loadings, or supports, are much bigger than the length scale of the microstructure. A classical boundary value problem is given in the following way:

$$\nabla\cdot\left(C\left(\frac{\vec{x}}{\tau}\right)\nabla u_\tau\right)=f \tag{98}$$

with τ being a very small parameter and $C(\vec{g})$ being a periodic coefficient $C(\vec{g}+\vec{e}_i)=C(\vec{g})$, i=1, …, n. It may be modified to the following form:

$$\nabla\cdot(C^*\nabla u)=f \tag{99}$$

where C^* is the effective constitutive tensor with constant coefficients representing a homogenized material. This property could be computed as

$$C^*_{ij}=\int_{(0,1)^n} C(\vec{g})(\nabla w_j(\vec{g})+\vec{e}_j)\cdot\vec{e}_i dy_1\ldots dy_n, \qquad i,j=1,\ldots,n \tag{100}$$

where periodic w_j satisfies $\nabla_y\cdot(C(\vec{g})\nabla w_j)=-\nabla_y\cdot(C(\vec{g})\vec{e}_j)$. One equation may be replaced by another if τ is small enough to satisfy $u_\tau\approx u$ and when $u_\tau\to u$ at $\tau\to 0$. Regarding the continuum concept, an analog of the differential element is the representative volume element (RVE) in 3D problems or the representative surface element (RSE) in 2D problems. This should be selected in a way to contain all the relevant statistical information about an inhomogeneous medium. With such an assumption, averaging over this element results in an effective property of the medium defined as C^* above. A key problem in such a formulation is the assumption that such an RVE is solvable and contains as much information about the microstructure as possible. This also holds for stochastic calculations where, in addition to the RVE selection, uncertain parameters must also be selected in a way to catch the best representation of the most important randomness sources and remain simple enough to be solved.

In its early approaches, homogenization was used in a purely analytical [233,242] way, and thus, the microstructure was very simple and the range of applications was limited. This obstacle was overcome with the incorporation of the FEM, where the RVE was modeled and solved. The rapid evolution of the academic and commercial FEM software that started at the end of the twentieth century supported researchers in the discretization and visualization of the RVE. A simultaneous revolution in the computational power of personal computers made solutions to more complex problems accessible. All of this allowed homogenization to become one of the most widespread methods used to solve multiscale problems in materials science, especially those connected to the meso- and microscale of inhomogeneous materials (see, e.g., [243–245]). The topic of a correct RVE is so important that some studies treat it as a research problem connected with its generation [246], size or scale effect [247–251], and validity of applied random microstructure [252]. Some other works reviewed existing stochastic boundary conditions and introduce new ones [253] or propose a formulation of finite elements for the hyper-elastic case [254]. The FEM is commonly included in approaches that are aimed at decreasing the problem size or computation time, which is done at the expense of accuracy. These propose the usage of artificial neural networks and machine learning approaches [255–257], divide the heterogeneous medium into several subdomains [117], use a manifold-learning method to reduce the dimensions of microscopic strain fields [258], utilize orthogonal decomposition R3M [259], or aim to apply a reduced database model [260], to name a few. The FEM is, of course, not the only possibility. There also exist

some alternative methods, such as mesh-free formulations [261], a gradient approach [262], fast Fourier transform (FFT)-based methods [263], a transformation field [264], or the discrete element method [265], which are perfect for densely packed solids. Sometimes, a nonlinear response of the material is studied, for which some approaches to homogenization exist, such as the ones in [266–269]. In many cases, they include specific a priori assumptions related to the stress or strain fields (see, e.g., [270–272]). Probabilistic homogenization adds yet one more level of abstraction to homogenization. It introduces uncertain parameters and variables in the lower scale of homogenization, usually in the material microstructure; some examples were presented and discussed in [273–279]. Similarly to probabilistic analysis in macroscopic calculations, it quantifies the influence of input uncertainty on the response of the medium. The difference is the source of uncertainty, which cannot be included at a macroscopic level, yet cause randomness in engineering structures. Common problems for which probabilistic homogenization is applied include uncertain phase properties, interface defects, geometric uncertainty, or inclusions. Uncertainty may be included in one phase or in in the various characteristics of the RVE, for example, the reinforcement positioning. They all result in an uncertain stiffness tensor or parameters leading to the material constitutive relation.

Probabilistic homogenization of composites is especially interesting when it is coupled with the problem of interface defects. An analytical solution to this problem can only be obtained for elastic composites and a simple RVE, which was proposed in [280]. A more in-depth analysis of the stiffness tensor, even in an elastic regime, requires the usage of numerical solvers. The author proposed such an approach [204], verified it with an analytical solution, and studied a fully anisotropic response of the homogenized composite [11]. The results demonstrated that particle clustering and uneven particle distribution affect the anisotropy of the composite and have a high influence on the components of its stiffness tensor. In his other work [8], he verified a numerical solution of a composite with an uncertain reinforcing particle radius with an analytical solution and studied an influence of an uncertain aspect ratio on the effective stiffness tensor of a composite. One may extend this model toward a hyper-elastic regime of the composite, where an uncertain hyper-elastic response of a homogeneous medium can be taken into account [115], which may be further extended toward the stochastic hyper-elastic response of composites with hysteresis [99] and with stochastic interface defects [281,282].

As it is well-known, the effective response of a medium is a relation of the objective function with uncertain parameters or variables. In structural design, the objective function could be defined as a limit function. In homogenization, it usually is an effective property of a medium, such as the stiffness tensor, bulk modulus, effective stress, or strain energy. In the majority of homogenization problems (and also in most structural engineering problems), such a relation cannot be analytically determined. This is a reason why the objective function is commonly computed with the use of discrete numerical procedures. In SPT, this is frequently done using a response function method (RFM) [138] or response surface method (RSM) [283,284] when more variables are considered. An alternative to the direct differentiation method (DDM) is rarely selected because it requires at least an intervention into a source code of a discrete numerical solver or even the introduction of its solver. This is because the deterministic values used by these programs must be substituted with their stochastic counterparts.

The response function method and the response surface method both aim to approximate the real relations of the objective function with the use of a surrogate model (also called a meta-model [285,286]) with an uncertain variable. This is done based on a carefully selected set of discrete numerical (or laboratory) experiments performed for different values of input variables [287,288]. Their major advantage is the ease of application and disconnection of the metamodel fitting from the stochastic procedure, which allows for a simple analysis of the fitting errors. Surrogate models are commonly applied from a subset of polynomial functions and also their fractions or other rational

functions [289,290]; a little less common is an application of the B-spline, logarithmic, exponential, or hyperbolic functions.

Searching for the response functions or surfaces is an optimization problem and can be solved using linear programming (LP), quadratic programming (QP), and nonlinear programming (NP) methods. A class of linear programming problems is one where the objective function and all of the constraints are linear functions of the decision variables. It always has either (a) one or more equivalent globally optimal solutions, (b) has an unbounded objective, or (c) no feasible solution. It is convex and has at most one feasible region with "flat faces" (i.e., no curves) on its outer surface. Its optimal solution (if available) lays at a "corner point" on this surface that is represented by constraints. A solver may work pointwise and the solution is fast. Common solvers include families of the simplex technique in its primal [291] or dual [292] version and the interior point technique [293], where the fitting procedure is completed with a linear or (sometimes) nonlinear version of the Least Squares Method.

As it is well known, a quadratic programming problem has an objective function that is a quadratic function of the design variables and constraints that are all linear functions of the variables. They have only one feasible region with "flat faces" on its surface (due to the linear constraints), but the optimal solution may be found anywhere within this region or on its surface. As it is well known, an objective function may be convex or non-convex. The convex functions have either positive definite or semi-definite Hessians, and non-convex have an indefinite Hessian and a saddle shape, which is usually out of the scope of QP solvers. Typical solvers include a simplex extension to the QP, active set and working set method variations [294,295], interior point [296–298], or Newton barrier methods [299–302]. A nonlinear programming problem similar to the hyper-elastic stochastic analysis of composites and their effective characteristics is no doubt one of the most difficult issues in optimization theory. An objective function is generally a nonlinear function of the decision variables and may have many locally optimal solutions. A global minimum is very difficult to be found [303], and common solvers include augmented Lagrange methods [304], sequential quadratic programming [305,306], and reduced gradient methods [307,308].

7. Concluding Remarks

As demonstrated in this review work, an application of probabilistic and stochastic methods in the analysis of hyper-elastic solids still attracts many researchers and has a large audience. Such an approach is especially very convenient for engineering practice with polymer-based composites, specifically elastomers. Experimental statistics included in new theoretical and computer models allow for further optimization of such materials. This may be crucial for the optimal design of structural dampers, whose reliability, durability, and structural health monitoring may bring huge qualitative and quantitative savings. Stochastic multiscale models, especially including the atomistic scale of the solid, are indeed still very scarce, mainly since this scale uncertainty requires relatively expensive Monte Carlo simulations to obtain reliable stochastic analyses. Time and computer power consumption in this case is still slowly decreasing, but this is the main reason to continuously look for some concurrent techniques. This is also why various homogenization methods remain very attractive in materials engineering, especially those accounting for material and geometrical imperfections of a random nature, and most probably will remain so in the future.

Author Contributions: Conceptualization: M.K.; methodology: M.K. and D.S.; formal analysis: M.K. and D.S.; investigation: M.K. and D.S.; writing – original draft preparation: M.K. and D.S.; writing – review and editing: M.K. and D.S.; supervision: M.K.; project administration: M.K.; funding acquisition: M.K. All authors have read and agreed to the published version of the manuscript.

Funding: The authors would like to acknowledge the financial support of the grant Preludium 2016/21/N/ST8/01224 sponsored by the National Science Center in Cracow, Poland, and the research grant OPUS no. 2021/41/B/ST8/02432 "Probabilistic entropy in engineering computations" sponsored by the same institution.

Institutional Review Board Statement: Not applicable.

Informed Consent Statement: Not applicable.

Data Availability Statement: Not applicable.

Conflicts of Interest: The Authors declare no conflict of interest.

References

1. Mark, J.E. *Physical Properties of Polymers Handbook*, 2nd ed.; Springer: New York, NY, USA, 2007.
2. Heinrich, G.; Klűppel, M.; Vilgis, T.A. Reinforcement of elastomers. *Curr. Opin. Solid State Mat. Sci.* **2002**, *6*, 195–203.
3. Vilgis, T.A.; Heinrich, G.; Klüppel, M. *Reinforcement of Polymer Nanocomposites: Theory, Experiment and Applications*; Cambridge University Press: Cambridge, UK, 2009.
4. Khalifa, M.; Anandhan, S.; Wuzella, G.; Lammer, H.; Mahendran, A.R. Thermoplastic polyurethane composites reinforced with renewable and sustainable fillers—A review. *Polym. Technol. Mater.* **2020**, *59*, 1751–1769.
5. Máša, B.; Náhlík, L.; Hutař, P. Particulate Composite Materials: Numerical Modeling of a Cross-Linked Polymer Reinforced With Alumina-Based Particles. *Polym. Mech.* **2013**, *49*, 421–428.
6. Delfani, M.; Bagherpour, V. Overall properties of particulate composites with periodic microstructure in second strain gradient theory of elasticity. *Mech. Mater.* **2017**, *113*, 89–101.
7. Fukahori, Y. The mechanics and mechanism of the carbon black reinforcement of elastomers. *Rubber Chem. Technol.* **2003**, *76*, 548–566.
8. Kamiński, M. Sensitivity analysis of homogenized charactersitics for random elastic composites. *Comput. Methods Appl. Mech. Eng.* **2003**, *192*, 1973–2005.
9. Kamiński, M.; Sokołowski, D. Dual probabilistic homogenization of the rubber-based composite with random carbon black particle reinforcement. *Comp. Struct.* **2016**, *140*, 783–797.
10. Fish, J.; Shek, K.; Pandheeradi, M.; Shephard, M.S. Computational plasticity for composite structures based on mathematical homogenization: Theory and practice. *Comput. Methods Appl. Mech. Eng.* **1997**, *148*, 53–73.
11. Sokołowski, D.; Kamiński, M. Homogenization of carbon/polymer composites with anisotropic distribution of particles and stochastic interface defects. *Acta Mech.* **2018**, *229*, 3727–3765.
12. Le, T.T.; Guilleminot, J.; Soize, C. Stochastic continuum modelling of random interphases from atomistic simulations. Application to a polymer nanocomposite. *Comput. Methods Appl. Mech. Eng.* **2016**, *303*, 430–449.
13. Clement, A.; Soize, C.; Yvonnet, J. Computational nonlinear stochastic homogenization using a non-concurrent multiscale approach for hyperelastic heterogeneous microstructures analysis. *Int. J. Numer. Methods Eng.* **2012**, *91*, 799–824.
14. Melchers, R.E. *Structural Reliability Analysis and Prediction*, 3rd ed.; Wiley: Chichester, UK, 2002. https://doi.org/10.1002/9781119266105.
15. Wang, X.; Xu, X.; Choi, S.U.S. Thermal conductivity of nanoparticle-fluid mixture. *J. Thermophys. Heat Transf.* **1999**, *13*, 474–480.
16. López-Pernía, C.; Muñoz-Ferreiro, C.; González-Orellana, C.; Morales-Rodríguez, A.; Gallardo-López, Á.; Poyato, R. Optimizing the homogenization technique for graphene nanoplatelet/yttria tetragonal zirconia composites: Influence on the microstructure and the electrical conductivity. **J. Alloy. Compd. 2018**, *767*, 994–1002.
17. Miehe, C.; Diez, J.; Goktepe, S.; Schanzel, L. Coupled thermovisco-elastoplasticity of glassy polymers in the logarithmic strain space based on the free volume theory. *Int. J. Sol. Struct.* **2011**, *48*, 1799–1817.
18. Christensen, R.M. *Mechanics of Composite Materials*; Wiley: New York, NY, USA, 1979.
19. Timoshenko, S.; Goodier, J.N. *Elasticity Theory*; McGraw-Hill: New York, NY, USA, 1951.
20. Zener, C. *Elasticity and Anelasticity of Metals*; University of Chicago: Chicago, IL, USA, 1948.
21. Humphrey, J.D. *Cardiovascular Solid Mechanics: Cells, Tissues and Organs*; Springer: New York, NY, USA, 2002.
22. Glotzer, S.C.; Paul, W. Molecular and Mesoscale Simulation Methods for Polymer Materials. *Annu. Rev. Mater. Sci.* **2002**, *32*, 401–436.
23. Bhowmick, A. *Current Topics in Elastomers Research*; CRC Press: Boca Raton, FL, USA, 2008.
24. Christensen, R.M. *Theory of Viscoelasticity*; Dover Publications: Dover, UK, 2010.
25. Attard, M.M.; Hunt, G.W. Hyperelastic constitutive modeling under finite strain. *Int. J. Solids Struct.* **2004**, *41*, 5327–5350.
26. Yang, B.; Kim, B.; Lee, H. Predictions of viscoelastic strain rate dependent behavior of fiber-reinforced polymeric composites. *Compos. Struct.* **2012**, *94*, 1420–1429.
27. Zhang, J.; Ostoja-Starzewski, M. Mesoscale bounds in viscoelasticity of random composites. *Mech. Res. Commun.* **2015**, *68*, 98–104.
28. Heinrich, G.; Struve, J.; Gerber, G. Mesoscopic simulation of dynamic crack propagation in rubber materials. *Polymer* **2002**, *43*, 395–401.

29. Harth, T.; Schwan, S.; Lehn, J.; Kollmann, F. Identification of material parameters for inelastic constitutive models: Statistical analysis and design of experiments. *Int. J. Plast.* **2004**, *20*, 1403–1440.
30. Mandel, J.; Roth, F.L.; Steel, M.N.; Stiehler, R.D. Measurement of the aging of rubber vulcanizates. *J. Res. Natl. Bur. Stand. Sect.—C. Eng. Instr.* **1959**, *63*, 141–145.
31. Mott, P.H.; Roland, C.M. Aging of natural rubber in air and seawater. *Rubber Chem. Technol.* **2001**, *74*, 79–88.
32. Mullins, L. Softening of rubber by deformation. *Rubber Chem. Technol.* **1969**, *42*, 339–362.
33. Ogden, R.; Roxburgh, D.G. A pseudo–elastic model for the Mullins effect in filled rubber. *Proc. R. Soc. A Math. Phys. Eng. Sci.* **1999**, *455*, 2861–2877.
34. Dorfmann, A.; Ogden, R. A constitutive model for the Mullins effect with permanent set in particle-reinforced rubber. *Int. J. Solids Struct.* **2004**, *41*, 1855–1878.
35. Lorenz, H.; Klüppel, M.; Heinrich, G. Microstructure-based modelling and FE implementation of filler-induced stress softening and hysteresis of reinforced rubbers. *ZAMM-J. Appl. Math. Mech.* **2012**, *92*, 608–631.
36. Volokh, K. On modeling failure of rubber-like materials. *Mech. Res. Commun.* **2010**, *37*, 684–689.
37. Volokh, K.Y. Review of the energy limiters approach to modeling failure of rubber. *Rubber Chem. Technol.* **2013**, *86*, 470–487.
38. Treloar, L.R. *The Physics of Rubber Elasticity*; Clarendon Press: Oxford, UK, 1975.
39. Heinrich, G.; Straube, E.; Helmis, G. Rubber elasticity of polymer networks: Theories. *Adv. Polymer Sci.* **1988**, *85*, 33–87.
40. Holzapfel, G.A. *Nonlinear Solid Mechanics: A Continuum Approach for Engineering*; Wiley: Chichester, UK, 2000.
41. Truesdell, C.; Noll, W. *The Non-Linear Field Theories of Mechanics*, 3rd ed.; Springer: Berlin/Heidelberg, Germany, 2004.
42. Sussman, T.; Bathe, K.-J. A finite element formulation for nonlinear incompressible elastic and inelastic analysis. *Comput. Struct.* **1987**, *26*, 357–409.
43. Heinrich, G.; Kaliske, M. Theoretical and numerical formulation of a molecular based constitutive tube-model of rubber elasticity. *Comput. Theor. Polym. Sci.* **1997**, *7*, 227–241.
44. Kaliske, M.; Rothert, H. On the finite element implementation of rubber-like materials at finite strains. *Eng. Comput.* **1997**, *14*, 216–232.
45. Jin, T.; Yu, L.; Yin, Z.; Xiao, H. Bounded elastic potentials for rubberlike materials with strain-stiffening effects. **2014**, *95*, 1230–1242.
46. Hossain, M.; Steinmann, P. More hyperelastic models for rubber-like materials: Consistent tangent operators and comparative study. *J. Mech. Behav. Mater.* **2013**, *22*, 27–50.
47. He, H.; Zhang, Q.; Chen, J.; Zhang, L.; Li, F. A comparative study of 85 hyperelastic constitutive models for both unfilled rubber and highly filled rubber nanocomposite material. *Nano Mater. Sci.* **2022**, *4*, 64–82.
48. Zopf, C.; Kaliske, M. Numerical characterisation of uncured elastomers by a neural network based approach. *Comput. Struct.* **2017**, *182*, 504–525.
49. Shen, Y.; Chandrashekhara, K.; Breig, W.F.; Oliver, L.R. Neural Network Based Constitutive Model for Rubber Material. *Rubber Chem. Technol.* **2004**, *77*, 257–277.
50. Klein, D.K.; Fernández, M.; Martin, R.J.; Neff, P.; Weeger, O. Polyconvex anisotropic hyperelasticity with neural networks. *J. Mech. Phys. Solids* **2022**, *159*, 104703.
51. Chung, I.; Im, S.; Cho, M. A neural network constitutive model for hyperelasticity based on molecular dynamics simulations. *Int. J. Numer. Methods Eng.* **2021**, *122*, 5–24.
52. Le, B.A.; Yvonnet, J.; He, Q.-C. Computational homogenization of nonlinear elastic materials using neural networks: Neural networks-based computational homogenization. *Int. J. Numer. Methods Eng.* **2015**, *104*, 1061–1084.
53. Mooney, M. A theory of large elastic deformation. *J. Appl. Phys.* **1940**, *11*, 582–592.
54. Rivlin, R.S. Large elastic deformations of isotropic materials. IV. Further developments of the general theory. *Phil. Trans. R. Soc. Lond. Ser. A Math. Phys. Sci.* **1948**, *241*, 379–397.
55. Ogden, R. On the overall moduli of non-linear elastic composite materials. *J. Mech. Phys. Solids* **1974**, *22*, 541–553.
56. Ogden, R.W. *Non-Linear Elastic Deformations*, Dover Publishers: Dover, UK, 1984.
57. Treloar, L. The elasticity of a network of long-chain molecules II. *Trans. Faraday Soc.* **1943**, *39*, 241–246.
58. Isihara, A.; Hashitsume, N.; Tatibana, M. Statistical theory of rubber-like elasticity. IV. (two-dimensional stretching). *J. Chem. Phys.* **1951**, *19*, 1508–1512.
59. Yeoh, O.H. Characterization of elastic properties of carbon-black-filled rubber vulcanizates. *Rubber Chem. Technol.* **1990**, *63*, 792–805.
60. Carroll, M.M. A strain energy function for vulcanized rubbers. *J. Elast.* **2010**, *103*, 173–187.
61. Melly, S.K.; Liu, L.; Liu, Y.; Leng, J. Improved Carroll's hyperelastic model considering compressibility and its finite element implementation. *Acta Mech. Sin.* **2021**, *37*, 785–796.
62. Zhao, Z.; Mu, X.; Du, F. Modeling and verification of a new hyperelastic model for rubber-like materials. *Math. Probl. Eng.* **2019**, *2019*, 2832059.
63. Knowles, J.K. The finite anti-plane shear field near the tip of a crack for a class of incompressible elastic solids. *Int. J. Fract.* **1977**, *13*, 611–639.
64. Swanson, S.R. A Constitutive Model for High Elongation Elastic Materials. *ASME J. Eng. Mater. Technol.* **1985**, *107*, 110–114.
65. Gregory, I.H.; Muhr, A.H.; Stephens, I.J. Engineering applications of rubber in simple extension. *Plast. Rubber Compos. Process. Appl.* **1997**, *26*, 118–122.

66. Lopez-Pamies, O. A new I1-based hyperelastic model for rubber elastic materials. **2010**, *338*, 3–11.
67. Yeoh, O.H. Some forms of the strain energy function for rubber. *Rubber Chem. Technol.* **1993**, *66*, 754–771.
68. Hohenberger, T.W.; Windslow, R.J.; Pugno, N.M.; Busfield, J.J.C. A constitutive model for both low and high strain nonlinearities in highly filled elastomers and implementation with user-defined material soubrutines in ABAQUS. *Rubber Chem. Technol.* **2019**, *92*, 653–686.
69. Gent, A.N.; Thomas, A. Forms for the stored (strain) energy function for vulcanized rubber. *J. Polym. Sci.* **1958**, *28*, 625–628.
70. Hart-Smith, L.J. Elasticity parameters for finite deformations of rubber-like materials. *Z. Angew. Math. Phys.* **1966**, *17*, 608–626.
71. Alexander, H. A constitutive relation for rubber-like materials. *Int, J. Eng. Sci.* **1968**, *6*, 549–563.
72. Hoss, L.; Marczak, R.J. A New Constitutive Model for Rubber-Like Materials. *Mecánica Comput.* **2010**, *29*, 2759–2773.
73. Khajehsaeid, H.; Arghavani, J.; Naghdabadi, R. A hyperelastic constitutive model for rubber-like materials. *Eur. J. Mech. A/Solids* **2013**, *38*, 144–151.
74. Anssari-Benam, A.; Bucchi, A. A generalised neo-Hookean strain energy function for application to the finite deformation of elastomers. *Int. J. Non-Linear Mech.* **2020**, *128*, 103626.
75. Warner, H.R., Jr. Kinetic theory and rheology of dilute suspensions of finitely extendible dumbbells. *Ind. Eng. Chem. Fundam.* **1972**, *11*, 379–387.
76. Kilian, H.-G. A molecular interpretation of the parameters of the van der Waals equation of state for real networks. *Polym. Bull.* **1980**, *3*, 151–158.
77. Gent, A.N. A new constitutive relation for rubber. *Rubber Chem. Technol.* **1996**, *69*, 59–61.
78. Pucci, E.; Saccomandi, G. A note on the Gent model for rubber-like materials. *Rubber Chem. Technol.* **2002**, *75*, 839–852.
79. Horgan, C.O.; Murphy, J.G. Limiting chain extensibility constitutive models of Valanis–Landel type. *J. Elast.* **2007**, *86*, 101–111.
80. Valanis, K.C.; Landel, R.F. The strain-energy function of a hyperelastic material in terms of the extension ratios. *J. Appl. Phys.* **1967**, *38*, 2997–3002.
81. Valanis, K.C. The Valanis–Landel strain energy function Elasticity of incompressible and compressible rubber-like materials. *Int. J. Solids Struct.* **2021**, *238*, 111271.
82. Narooei, K.; Arman, M. Modification of exponential based hyperelastic strain energy to consider free stress initial configuration and Constitutive modeling. *J. Comput. Appl. Mech.* **2018**, *49*, 189–196.
83. Beda, T.; Chevalier, Y. Hybrid continuum model for large elastic deformation of rubber. *J. Appl. Phys.* **2003**, *94*, 2701–2706.
84. Korba, A.G.; Barkey, M.E. New model for hyper-elastic materials behavior with an application on natural rubber. In Proceedings of the ASME 2017 12th International Manufacturing Science and Engineering Conference Collocated with the JSME/ASME 2017 6th International Conference on Materials and Processing, American Society of Mechanical Engineers Digital Collection, Los Angeles, CA, USA, 4–8 June 2017; pp. 1–10.
85. Treloar, L. The elasticity of a network of long-chain molecules. I. *Trans. Faraday Soc.* **1943**, *39*, 36–41.
86. Ball, R.; Doi, M.; Edwards, S.; Warner, M. Elasticity of entangled networks. *Polymer* **1981**, *22*, 1010–1018.
87. Rubinstein, M.; Panyukov, S. Nonaffine deformation and elasticity of polymer networks. *Macromolecules* **1997**, *30*, 8036–8044.
88. James, H.M.; Guth, E. Theory of the elastic properties of rubber. *J. Chem. Phys.* **1943**, *11*, 455–481.
89. Arruda, E.M.; Boyce, M.C. A three-dimensional constitutive model for the large stretch behavior of rubber elastic materials. *J. Mech. Phys. Solids* **1993**, *41*, 389–412.
90. Boehler, J.-P.; Khan, A.S. (Eds.) *Anisotropy and Localization of Plastic Deformation*; Springer: Berlin/Heidelberg, Germany, 1991.
91. Song, D.; Oberai, A.A.; Janmey, P.A. Hyperelastic continuum models for isotropic athermal fibrous networks. *Interface Focus* **2022**, *12*, 20220043.
92. Flory, P.J. Thermodynamic relations for high elastic materials. *Trans. Faraday Soc.* **1961**, *57*, 829–838.
93. Miehe, C.; Göktepe, S.; Lulei, F. A micro-macro approach to rubber-like materials—Part I: The non-affine micro-sphere model of rubber elasticity. *J. Mech. Phys. Solids* **2004**, *52*, 2617–2660.
94. Kaliske, M.; Heinrich, G. An extended tube-model for rubber elasticity: Statistical-mechanical theory and finite element implementation. *Rubber Chem. Technol.* **2010**, *72*, 602–632.
95. Khiêm, V.N.; Itskov, M. Analytical network-averaging of the tube model: Rubber elasticity. *J. Mech. Phys. Solid.* **2016**, *95*, 254–269.
96. Xiang, Y.; Zhong, D.; Wang, P.; Mao, G.; Yu, H.; Qu, S. A general constitutive model of soft elastomers. *J. Mech. Phys. Solids* **2018**, *117*, 110–122.
97. Wu, P.; van der Giessen, E. On improved 3-D non-Gaussian network models for rubber elasticity. *Mech. Res. Commun.* **1992**, *19*, 427–433.
98. Lim, G.T. Scratch Behavior of Polymers; Texas A&M University: College Station, TX, USA, 2005.
99. Bechir, H.; Chevalier, L.; Idjeri, M. A three-dimensional network model for rubber elasticity: The effect of local entanglements constraints. *Int. J. Eng. Sci.* **2010**, *48*, 265–274.
100. Elhaouzi, F.; Nourdine, A.; Brosseau, C.; Mdarhri, A.; El Aboudi, I.; Zaghrioui, M. Hyperelastic behavior and dynamic mechanical relaxation in carbon black-polymer composites. *Polym. Compos.* **2018**, *40*, 3005–3011.
101. Fritzen, F.; Kunc, O. Two-stage data-driven homogenization for nonlinear solids using a reduced order model. *Eur. J. Mech. A/Solids* **2018**, *69*, 201–220.
102. Li, X.; Xia, Y.; Li, Z.; Xia, Y. Three-dimensional numerical simulations on the hyperelastic behavior of carbon-black particle filled rubbers under moderate finite deformation. *Comput. Mater. Sci.* **2012**, *55*, 157–165.

103. Shahabodini, A.; Ansari, R.; Darvizeh, M. Multiscale modeling of embedded graphene sheets based on the higher-order Cauchy-Born rule: Nonlinear static analysis. *Compos. Struct.* **2017**, *165*, 25–43.
104. Temizer, I.; Zohdi, T.I. A numerical method for homogenization in non-linear elasticity. *Comput. Mech.* **2007**, *40*, 281–298. https://doi.org/10.1007/s00466-006-0097-y.
105. Sokołowski, D.; Kamiński, M. Hysteretic behavior of random particulate composites by the Stochastic Finite Element Method. *Materials* **2019**, *12*, 2909.
106. Leonard, M.; Wang, N.; Lopez-Pamies, O.; Nakamura, T. The nonlinear elastic response of filled elastomers: Experiments vs. theory for the basic case of particulate fillers of micrometer size. *J. Mech. Phys. Solids* **2019**, *135*, 103781.
107. Jiménez, F.L. Variations in the distribution of local strain energy within different realizations of a representative volume element. *Compos. Part B Eng.* **2019**, *176*, 107111.
108. Ban, Y.; Mi, C. On spherical nanoinhomogeneity embedded in a half-space analyzedwith Steigmann–Ogden surface and interface models. *Int. J. Solids Struct.* **2021**, *216*, 123–135.
109. Pallicity, T.D.; Böhlke, T. Effective viscoelastic behavior of polymer composites with regularperiodic microstructures. *Int. J. Solids Struct.* **2021**, *216*, 167–181.
110. Avril, S.; Badel, P.; Duprey, A. Anisotropic and hyperelastic identification of in vitro human arteries from full-field optical measurements. *J. Biomech.* **2010**, *43*, 2978–2985.
111. Sakata, S.; Ashida, F.; Kojima, T.; Zako, M. Three-dimensional stochastic analysis using a perturbation based homogenization metod for elastic properties of composite material considering microscopic uncertainty. *Int. J. Solids Struct.* **2007**, *45*, 894–907.
112. Kalamkarov, A.L.; Kolpakov, A.G. *Analysis, Design and Optimization of Composite Structures*; Wiley: New York, NY, USA, 1997.
113. Guedri, M.; Lima, A.; Bouhaddi, N.; Rade, D. Robust design of viscoelastic structures based on stochastic finite element models. *Mech. Syst. Signal Process.* **2010**, *24*, 59–77.
114. Nezamabadi, S.; Zahrouni, H.; Yvonnet, J. Solving hyperelastic material problems by asymptotic numerical method. *Comput. Mech.* **2010**, *47*, 77–92.
115. Kamiński, M.; Sokołowski, D. An introduction to stochastic finite element method analysis of hyper-elastic structures. In Proceedings of the 7th European Congress on Computational Methods in Applied Sciences and Engineering, Crete, Greece, 5–10 June 2016; Volume 3, pp. 6078–6090; ISSN 00002016.
116. Zeraatpisheh, M.; Bordas, S.P.; Beex, L.A. Bayesian model uncertainty quantification for hyperelastic soft tissue models. *Data-Cent. Eng.* **2021**, *2*, e9.
117. Liu, Z.; Bessa, M.; Liu, W.K. Self-consistent clustering analysis: An efficient multi-scale scheme for inelastic heterogeneous materials. *Comput. Methods Appl. Mech. Eng.* **2016**, *306*, 319–341.
118. Staber, B.; Guilleminot, J. Stochastic hyperelastic constitutive laws and identification procedure for soft biological tissues with intrinsic variability. *J. Mech. Behav. Biomed. Mater.* **2017**, *65*, 743–752.
119. Staber, B.; Guilleminot, J. Stochastic modeling of the Ogden class of stored energy functions for hyperelastic materials: The compressible case. *Z. Angew. Math. Mech.* **2017**, *97*, 273–295.
120. Lopez-Pamies, O.; Idiart, M.I. Fiber-reinforced hyperelastic solids: A realizable homogenization constitutive theory. *J. Eng. Math.* **2010**, *68*, 57–83.
121. López Jiménez, F. Modeling of soft composites under three-dimensional loading. **Compos. Part B Eng. 2014**, *59*, 173–180.
122. Staber, B.; Guilleminot, J. Functional approximation and projection of stored energy functions in computational homogenization of hyperelastic materials: A probabilistic perspective. *Comput. Method. Appl. Mech.* **2017**, *313*, 1–27.
123. Ghaboussi, J.; Garrett, J.H.; Wu, X. Knowledge-Based Modeling of Material Behavior with Neural Networks. *J. Eng. Mech.* **1991**, *117*, 132–153.
124. Karniadakis, G.E.; Kevrekidis, I.G.; Lu, L.; Perdikaris, P.; Wang, S.; Yang, L. Physics-informed machine learning. *Nat. Rev. Phys.* **2021**, *3*, 422–440.
125. As'ad, F.; Avery, P.; Farhat, C. A mechanics-informed artificial neural network approach in data-driven constitutive modeling. Intenat. *J. Numer. Methods Eng.* **2022**, *123*, 2738–2759.
126. Mahnken, R. Strain mode-dependent weighting functions in hyperelasticity accounting for verification, validation, and stability of material parameters. *Arch. Appl. Mech.* **2022**, *92*, 713–754.
127. Linka, K.; Kuhl, E. A new family of Constitutive Artificial Neural Networks towards automated model discovery. *Comput. Methods Appl. Mech. Eng.* **2023**, *403*, 115731.
128. Kalina, K.A.; Linden, L.; Brummund, J.; Metsch, P.; Kästner, M. Automated constitutive modeling of isotropic hyperelasticity based on artificial neural networks. *Comput. Mech.* **2021**, *69*, 213–232.
129. Hien, T.D.; Kleiber, M. On solving nonlinear transient heat transfer problems with random parameters. *Comput. Methods Appl. Mech. Eng.* **1998**, *151*, 287–299.
130. Xiu, D.; Karniadakis, G.E. A new stochastic approach to transient heat conduction modeling with uncertainty. *Int. J. Heat Mass Transf.* **2003**, *46*, 4681–4693. https://doi.org/10.1016/S0017-9310(03)00299-0.
131. Figiel, Ł.; Kamiński, M. Numerical probabilistic approach to sensitivity analysis in a fatigue delamination problem of a two-layer composite. *Appl. Math. Comput.* **2009**, *209*, 75–90.
132. Kamiski, M. On probabilistic fatigue models for composite materials. *Int. J. Fatigue* **2002**, *24*, 477–495.
133. Mustafa, G.; Suleman, A.; Crawford, C. Probabilistic micromechanical analysis of composite material stiffness properties for a wind turbine blade. *Compos. Struct.* **2015**, *131*, 905–916.

134. Vořehovský, M. Incorporation of statistical length scale into Weibull strength theory for composites. *Compos. Struct.* **2010**, *92*, 2027–2034.
135. Karakoç, A.; Freud, J. A statistical failure initiation model for honeycomb materials. *Compos. Struct.* **2013**, *95*, 154–162.
136. Ghaderi, A.; Morovati, V.; Dargazany, R. A Bayesian surrogate constitutive model to estimate failure probability of elastomers. *Mech. Mater.* **2021**, *162*, 104044.
137. Martínez-Frutos, J.; Ortigosa, R.; Pedregal, P.; Periago, F. Robust optimal control of stochastic hyperelastic materials. *Appl. Math. Model.* **2020**, *88*, 888–904.
138. Kamiński, M.M. **The Stochastic Perturbation Method for Computational Mechanics**; Wiley: Chichester, UK, 2013; ISBN 9780470770825.
139. Kamiński, M. On semi-analytical probabilistic finite element method for homogenization of the periodic fiber-reinforced composites. *Int. J. Numer. Methods Eng.* **2011**, *86*, 1144–1162.
140. Cruz, M.E.; Patera, A.T. A parallel Monte-Carlo finite-element procedure for the analysis of multicomponent random media. *Int. J. Numer. Methods Eng.* **1995**, *38*, 1087–1121.
141. Hurtado, J.E. Reanalysis of linear and nonlinear structures using iterated Shanks transformation. *Comput. Methods Appl. Mech. Eng.* **2002**, *191*, 4215–4229.
142. Hurtado, J.E.; Barbat, A.H. Monte Carlo techniques in computational stochastic mechanics. *Arch. Comput. Methods Eng.* **1998**, *5*, 3–29.
143. Hamada, M.; Wilson, A.; Reese, C.; Martz, H. *Bayesian Reliability*; Springer: Berlin/Heidelberg, Germany, 2008.
144. Lunn, D.J.; Thomas, A.; Best, N.; Spiegelhalter, D. WinBUGS—A Bayesian modelling framework: Concepts, structure, and extensibility. *Stat. & Comput.* **2000**, *10*, 325–337.
145. Zimmermann, H. Fuzzy set theory. *Wiley Interdiscip. Rev. Comput. Stat.* **2010**, *2*, 317–332.
146. Metropolis, N.; Ulam, S. The Monte Carlo Method. *J. Am. Stat. Assoc.* **1949**, *44*, 335–341. https://doi.org/10.1080/01621459.1949.10483310.
147. Hastings, W.K. Monte-Carlo sampling methods using Markov chains and their applications. *Biometrika* **1970**, *57*, 97–109.
148. Bendat, J.S.; Piersol, A.G. *Random Data: Analysis and Measurement Procedures*; Wiley: New York, NY, USA, 1971.
149. Doucet, A.; Godsill, S.; Andrieu, C. On sequential Monte Carlo sampling methods for Bayesian filtering. *Stat. Comput.* **2000**, *10*, 197–208.
150. Wilkinson, S.N.; Olley, J.M.; Furuichi, T.; Burton, J.; Kinsey-Henderson, A.E. Sediment source tracing with stratified sampling and weightings based on spatial gradients in soil erosion. *J. Soils Sediments* **2015**, *15*, 2038–2051.
151. Helton, J.C.; Davis, F.J. Latin hypercube sampling and the propagation of uncertainty in analyses of complex systems. *Reliab. Eng. Syst. Saf.* **2003**, *81*, 23–69.
152. Chung, D.B.; Gutiérrez, M.A.; Graham-Brady, L.L.; Lingen, F.-J. Efficient numerical strategies for spectral stochastic finite element models. *Int. J. Numer. Methods Eng.* **2005**, *64*, 1334–1349. https://doi.org/10.1002/nme.1404.
153. Ghanem, R.G.; Spanos, P.D. *Stochastic Finite Elements: A Spectral Approach*; Springer: Berlin/Heidelberg, Germany, 1991.
154. Ghanem, R.G.; Spanos, P.D. Spectral techniques for stochastic finite elements. *Arch. Comput. Methods Eng.* **1997**, *4*, 63–100. https://doi.org/10.1007/BF02818931.
155. Sasikumar, P.; Venketeswaran, A.; Suresh, R.; Gupta, S. A data driven polynomial chaos based approach for stochastic analysis of CFRP laminated composite plates. *Compos. Struct.* **2015**, *125*, 212–227.
156. Blatman, G.; Sudret, B. An adaptive algorithm to build up sparse polynomial chaos expansions for stochastic finite element analysis. *Probabilistic Eng. Mech.* **2010**, *25*, 183–197. https://doi.org/10.1016/j.probengmech.2009.10.003.
157. Tootkaboni, M.; Graham-Brady, L. A multi-scale spectral stochastic method for homogenization of multi-phase periodic composites with random material properties. *Int. J. Numer. Methods Eng.* **2010**, *83*, 59–90.
158. Xu, X.; Graham-Brady, L. A stochastic computational method for evaluation of global and local behavior of random elastic media. *Comput. Methods Appl. Mech. Eng.* **2005**, *194*, 4362–4385. https://doi.org/10.1016/j.cma.2004.12.001.
159. Kleiber, M.; Hien, T.D. *The Stochastic Finite Element Method*; Wiley: Chichester, UK, 1992.
160. Liu, W.K.; Belytschko, T.; Mani, A. Random field finite elements. *Int. J. Numer. Methods Eng.* **1986**, *23*, 1831–1845. https://doi.org/10.1002/nme.1620231004.
161. Matthies, H.G.; Brenner, C.E.; Bucher, C.G.; Soares, C.G. Uncertainties in probabilistic numerical analysis of structures and solids-Stochastic finite elements. *Struct. Saf.* **1997**, *19*, 283–336. https://doi.org/10.1016/S0167-4730(97)00013-1.
162. Stefanou, G.; Papadrakakis, M. Stochastic finite element analysis of shells with combined random material and geometric properties. *Comput. Methods Appl. Mech. Eng.* **2004**, *193*, 139–160, 2004. https://doi.org/10.1016/j.cma.2003.10.001.
163. Stefanou, G.; Savvas, D.; Papadrakakis, M. Stochastic finite element analysis of composite structures based on material microstructure. *Compos. Struct.* **2015**, *132*, 384–392.
164. Sasikumar, P.; Suresh, R.; Gupta, S. Analysis of CFRP laminated plates with spatially varying non-Gaussian inhomogeneities using SFEM. *Compos. Struct.* **2014**, *112*, 308–326.
165. Honda, R. Stochastic BEM with spectral approach in elastostatic and elastodynamic problems with geometrical uncertainty. *Eng. Anal. Bound. Elements* **2005**, *29*, 415–427. https://doi.org/10.1016/j.enganabound.2005.01.007.
166. Kaminski, M. Iterative scheme in determination of the probabilistic moments of the structural response in the Stochastic perturbation-based Boundary Element Method. *Comput. Struct.* **2015**, *151*, 86–95. https://doi.org/10.1016/j.compstruc.2015.01.017.

167. Wang, C.; Qiu, Z.; Wu, D. Numerical analysis of uncertain temperature field by stochastic finite difference method. *Sci. China Ser. G Phys. Mech. Astron.* **2014**, *57*, 698–707. https://doi.org/10.1007/s11433-013-5235-x.
168. Zienkiewicz, O.; Taylor, R.; Zhu, J. *The Finite Element Method Set. Its Basis and Fundamentals*, 6th ed.; Elsevier: Amsterdam, The Netherlands, 2005.
169. Ho, H.; Drzal, L.T. Evaluation of interfacial mechanical properties of fiber reinforced composites using the micro-indentation method. *Comp. Part A* **1996**, *27*, 961–971.
170. Zavarise, G.; Wriggers, P.; Stein, E.; Schrefler, B. A numerical model for thermomechanical contact based on microscopic interface laws. *Mech. Res. Commun.* **1992**, *19*, 173–182.
171. Khurshudyan, A.Z. The meso-scale behavior of anisotropic particle-reinforcedthermo-elastic composites. *Contin. Mech. Thermodyn.* **2021**, *33*, 1363–1374.
172. Chang, C.S.; Chao, S.J.; Chang, Y. Estimates of elastic moduli for granular material with anisotropic random packing structure. *Int. J. Solids Struct.* **1995**, *32*, 1989–2008.
173. Benveniste, Y. The effective mechanical behavior of composite material with imperfect contact between the constituents. *Mech. Mater.* **1985**, *4*, 197–208.
174. Firooz, S.; Javili, A. Understanding the role of general interfaces in the overall behavior of composites and size effects. *Comput. Mater. Sci.* **2019**, *162*, 245–254.
175. Lamon, J. Interfaces and Interphases. In *Ceramic Matrix Composites: Fiber Reinforced Ceramics and Their Applications*; Krenkel, W., Weinheim, E. Eds.; Wiley: Hoboken, NJ, USA, 2008, pp. 169–179.
176. Soize, C. Tensor-valued random fields for meso-scale stochastic model of anisotropic elastic microstructure and probabilistic analysis of representative volume element size. *Probabilistic Eng. Mech.* **2008**, *23*, 307–323.
177. Yang, B.; Hwang, Y.; Lee, H. Elastoplastic modeling of polymeric composites containing randomly located nanoparticles with an interface effect. *Compos. Struct.* **2013**, *99*, 123–130.
178. Choi, H.; Achenbach, J. Stress states at neighboring fibers induced by single-fiber interphase defects. *Int. J. Solids Struct.* **1995**, *32*, 1555–1570.
179. Goudarzi, T.; Spring, D.W.; Paulino, G.H.; Lopez-Pamies, O. Filled elastomers: A theory of filler reinforcement based on hydrodynamic and interphasial effects. J. Mech. and Phys. *Solids* **2015**, *80*, 37–67.
180. Meddeb, A.B.; Tighe, T.; Ounaies, Z.; Lopez-Pamies, O. Extreme enhancement of the nonlinear elastic response of elastomer nanoparticulate composites via interphases. *Compos. Part B Eng.* **2018**, *156*, 166–173.
181. Paran, S.M.R.; Saeb, M.R.; Formela, K.; Goodarzi, V.; Vijayan, P.P.; Puglia, D.; Khonakdar, H.A.; Thomas, S. To what extent can hyperelastic models make sense the effect of clay surface treatment on the mechanical properties of elastomeric nanocomposites? *Macromol. Mater. Eng.* **2017**, *302*, 1700036.
182. Qu, M.; Deng, F.; Kalkhoran, S.M.; Gouldstone, A.; Robisson, A.; Van Vliet, K.J. Nanoscale visualisation and multiscale mechanical implications of bound rubber interphases in rubber-carbon black nanocomposites. *J. Soft Matter* **2011**, *7*, 1066–1077.
183. Bismarck, A.; Blaker, J.; Anthony, D.; Qian, H.; Maples, H.; Robinson, P.; Shaffer, M.; Greenhalgh, E.; Anthony, D. Development of novel composites through fibre and interface/interphase modification. *IOP Conf. Ser. Mater. Sci. Eng.* **2016**, *139*, 012001. https://doi.org/10.1088/1757-899X/139/1/012001.
184. Livanov, K.; Yang, L.; Nissenbaum, A.; Wagner, H.D. Interphase tuning for stronger and tougher composites. *Sci. Rep.* **2016**, *6*, 26305. https://doi.org/10.1038/srep26305.
185. Shang-Lin, G.; Mäder, E. Characterization of interphase nanoscale property variation in glass fiber reinforced polypropylene and epoxy resin composites. *Comp. Part A Appl. Sci. Manuf.* **2002**, *33*, 559–576.
186. Kamiński, M.; Kleiber, M. Stochastic structural interface defects in fiber composites. *Int. J. Solids Struct.* **1996**, *33*, 3035–3056.
187. Le Duigou, A.; Davies, P.; Baley, C. Exploring durability of interfaces in flax fibre/epoxy micro-composites. *Compos. Part Ad Appl. Sci. Manuf.* **2013**, *48*, 121–128.
188. Beckmann, C.; Hohe, J. Effects of material uncertainty in the structural response of metal foam core sandwich beams. *Compos. Struct.* **2014**, *113*, 382–395.
189. Koutsawa, Y.; Karatrantos, A.; Yu, W.; Ruch, D. A micromechanics approach for the effective thermal conductivity of composite materials with general linear imperfect interfaces. *Compos. Struct.* **2018**, *200*, 747–756. https://doi.org/10.1016/j.compstruct.2018.05.113.
190. Whitehouse, A.F.; Clyne, T.W. Effects of reinforcement contact and shape on cavitation and failure in metal-matrix composites. *Composites* **1993**, *24*, 256–261.
191. Nazarenko, L.; Stolarski, H.; Altenbach, H. A statistical interphase damage model of random particulate composites. *Int. J. Plast.* **2019**, *116*, 118–142.
192. Reincke, K.; Grellmann, W.; Heinrich, G. Investigation of mechanical and fracture mechanical properties of elastomers filled with precipitated silica and nanofillers based upon layered silicates. *Rubber Chem. Technol.* **2004**, *77*, 662–677.
193. Golanski, D.; Terada, K.; Kikuchi, N. Macro and micro scale modeling of thermal residual stresses in metal matrix composite surface layers by the homogenization method. *Comput. Mech.* **1997**, *19*, 188–202.
194. Mura, T. **Micromechanics of Defects in Solids**; Springer Science & Business Media: Dordrecht, The Netherlands, 1987; ISBN 978-90-247-3256-2.
195. Hashin, Z. Thermoelastic properties of fiber composites with imperfect interface. *Mech. Mater.* **1990**, *8*, 333–348.

196. Theocaris, P.S. Definition of interphase in composites. In *The role of the Polymeric Matrix in the Processing and Structural Properties of Composite Materials*; Seferis, J.C., Nicolais, L., Eds.; Springer Science & Business Media: New York, NY, USA, 1983.
197. Yanase, K.; Ju, J.W. Effective elastic moduli of spherical particle reinforced composites containing imperfect interfaces. *Int. J. Damage Mech.* **2011**, *21*, 97–127.
198. Wu-Gui, J.; Ren-Zhi, Z.; Quing, H.; Yong-Gang, T. Homogenized finite element analysis on effective elastoplastic mechanical behaviors of composite with imperfect interfaces. *Int. J. Mol. Sci.* **2014**, *15*, 23389–23407.
199. Yanase, K.; Ju, J. Overall elastoplastic damage responses of spherical particle-reinforced composites containing imperfect interfaces. *Int. J. Damage Mech.* **2013**, *23*, 411–429.
200. Hashin, Z. The spherical inclusion with imperfect interface conditions. *J. Appl. Mech.* **1991**, *58*, 444–449.
201. Hashin, Z. Thin interphase/imperfect interface in elasticity with application to coated fiber composites. *J. Mech. Phys. Solids* **2002**, *50*, 2509–2537, 2002. https://doi.org/10.1016/S0022-5096(02)00050-9.
202. Jesson, A.D.; Watts, J.F. The interface and interphase in polymer matrix composites: Effect on mechanical properties and methods for identification. *Polym. Rev.* **2012**, *52*, 321–354.
203. Ručevskis, S.; Čate, A., Reichhold, J.; Błędzki, A.; Effective elastic constants of fiber-reinforced polymer-matrix composites with the concept of interphase. *Int. J. Appl. Mech. Engrg.* **2003**, *8*, 109-115.
204. Sokołowski, D.; Kamiński, M. Computational homogenization of carbon/polymer composites with stochastic interface defects. *Compos. Struct.* **2018**, *183*, 434.
205. Barulich, N.D.; Godoy, L.A.; Dardati, P.M. A computational micromechanics approach to evaluate elastic properties of composites with fiber-matrix interface damage. *Compos. Struct.* **2016**, *154*, 309–318.
206. Schellekens, J.C.; de Borst, R. The application of interface elements and enriched or rate-dependent continua to micro-mechanical analyses of fracture in composites. *Comput. Mech.* **1994**, *14*, 68–83.
207. Gutiérrez, M.A.; de Borst, R. Numerical analysis of localization using a viscoplastic regularization: Influence of stochastic material defects. *Int. J. Numer. Methods Eng.* **1999**, *44*, 1823–1841.
208. Géhant, S.; Fond, C.; Schirrer, R. Criteria for cavitation of rubber particles: Influence of plastic yielding in the matrix. *Int. J. Fract.* **2003**, *122*, 161–175.
209. Gurtin, M.E. *An Introduction to Continuum Mechanics*; Academic Press: Pittsburgh, PE, USA, 1982.
210. Kevrekidis, I.G.; Gear, C.W.; Hyman, J.M.; Kevrekidis, P.G.; Runborg, O.; Theodoropoulos, C. Equation-free, coarse-grained multiscale computation: Enabling microscopic simulators to perform system-level analysis. *Commun. Math. Sci.* **2003**, *1*, 715–762.
211. Jeulin, D.; Ostoja-Starzewski, M. (Eds.) *Mechanics of Random and Multiscale Structures*; CISM Courses and Lectures No. 430; Springer: New York, NY, USA, 2001.
212. Flores, E.S.; DiazDelaO, F.; Friswell, M.; Sienz, J. A computational multi-scale approach for the stochastic mechanical response of foam-filled honeycomb cores. *Compos. Struct.* **2011**, *94*, 1861–1870.
213. Bungartz, H.J.; Griebel, M. Sparse grids. *Acta Numer.* **2004**, *13*, 147–269.
214. Garcia-Cervera, C.; Ren, W.; Lu, J. Sequential multiscale modeling using sparse representation. *Commun. Comput. Phys.* **2008**, *4*, 1025–1033.
215. Tasan, C.C.; Hoefnagels, J.P.; Diehl, M.; Yan, D.; Roters, F.; Raabe, D. Strain localization and damage in dual phase steels investigated by coupledin-situde formation experiments and crystalplasticity simulations. *Int. J. Plast.* **2014**, *63*, 198–221.
216. Roters, F.; Eisenlohr, P.; Hantcherli, L.; Tjahjanto, D.D.; Bieler, T.R.; Raabe, D. Overview of constitutive laws, kinematics, homogenization and multiscale methods in crystal plasticity finite-element modeling: Theory, experiments, applications. *Acta Mat.* **2010**, *58*, 1152–1211.
217. Cusatis, G.; Rezakhani, R.; Alnaggar, M.; Zhou, Z.; Pelessone, D. Multiscale computational models for the simulation of concrete materials and structures. In *Proceedings of EURO-C 2014, Computational Modelling of Concrete and Concrete Structures*; Bicanic, N.; Mang, H.; Meschke, G.; de Borst, R.; Eds.; CRC Press/Taylor & Francis Group, 2014, pp. 23–38.
218. Kanouté, P.; Boso, D.P.; Chaboche, J.L.; Schrefler, B.A. Multiscale methods for composites: A review. *Arch. Comput. Methods Eng.* **2009**, *16*, 31–75. https://doi.org/10.1007/s11831-008-9028-8.
219. Brandt, A. Scientific Computation: Review. In *Multiscale and Multiresolution Methods: Theory and Applications, Yosemite Educational Symposium Conf. Proc.*; Barth, T.J., Ed.; Springer: Berlin/Heidelberg, Germany, 2001, ch. 20, pp. 3–96.
220. Weinan, E.; Engquist, B. The heterogeneous multi-scale methods. *Commun. Math. Sci.* **2003**, *1*, 87–133.
221. Ruban, A.I. *Fluid Dynamics Part 2: Asymptotic Problems of Fluid Dynamics*; Oxford University Press: Oxford, UK, 2015.
222. Kevorkian, J.; Cole, J.D. *Perturbation Methods in Applied Mathematics*; Springer: Berlin/Heidelberg, Germany, 1981.
223. Zhao, J.; Li, H.; Cheng, G.; Cai, Y. On predicting the effective elastic properties of polymer nanocomposites by novel numerical implementation of asymptotic homogenization method. *Compos. Struct.* **2016**, *135*, 297–305,.
224. Arnold, V.I. *Geometrical Methods in the Theory of Ordinary Differential Equations*; Springer: New York, NY, USA, 1983.
225. Kushnevsky, V.; Morachkovsky, O.; Altenbach, H. Identification of effective properties of particle reinforced composite materials. *Comput. Mech.* **1988**, *22*, 317–325.
226. Spohn, H. *Large Scale Dynamics of Interacting Particles*; Springer: New York, NY, USA, 1991.
227. Zwanzig, R.W. Collision of a Gas Atom with a Cold Surface. *J. Chem. Phys.* **1960**, *32*, 1173–1177.
228. Wilson, K.G.; Kogut, J. The renormalization group and the ε expansion. *Phys. Rep.* **1974**, *12*, 75–200.

229. Hashin, Z.; Shtrikman, S. A variational approach to the theory of the elastic behaviour of multiphase materials. *J. Mech. Phys. Solids* **1963**, *11*, 127–140.
230. Bensoussan, A.; Lions, J.L.; Papanicolaou, G. *Asymptotic Analysis for Periodic Structures*; North-Holland, Amsterdam, The Netherland, 1978.
231. Fish, J.; Chen, W. Higher-Order Homogenization of Initial/Boundary-Value Problem. *J. Eng. Mech.* **2001**, *127*, 1223–1230.
232. Ghosh, S.; Lee, K.; Moorthy, S. Multiple scale analysis of heterogeneous elastic structures using homogenization theory and voronoi cell finite element method. *Int. J. Solids Struct.* **1995**, *32*, 27–62.
233. Kamiński, M. *Computational Mechanics of Composite Materials*; Springer: London, UK; New York, NY, USA, 2005.
234. Wang, M.; Zhang, K.; Chen, C. A mixed FFT-Galerkin approach for incompressible or slightly compressible hyperelastic solids under finite deformation. *Comput. Methods Appl. Mech. Eng.* **2022**, *396*, 115092.
235. Zhang, G.; Feng, N.; Khandelwal, K. A computational framework for homogenization and multiscale stability analyses of nonlinear periodic materials. *Int. J. Numer. Methods Eng.* **2021**, *122*, 6527–6575.
236. Fernández, M.; Jamshidian, M.; Böhlke, T.; Kersting, K.; Weeger, O. Anisotropic hyperelastic constitutive models for finite deformations combining material theory and data-driven approaches with application to cubic lattice metamaterials. *Comput. Mech.* **2020**, *67*, 653–677.
237. Brändel, M.; Brands, D.; Maike, S.; Rheinbach, O.; Schröder, J.; Schwarz, A.; Stoyan, D. Effective hyperelastic material parameters from microstructures constructed using the planar Boolean model. *Comput. Mech.* **2022**, *69*, 1295–1321.
238. Somoh, G.K.; Ben Toumi, R.; Renard, J.; Monin, M. Statistical approach of elastic properties of continuous fiber composite. *Compos. Struct.* **2015**, *119*, 287–297.
239. Milton, G.W. *The Theory of Composites*; Cambridge University Press: Cambridge, UK, 2002.
240. Fu, S.-Y.; Lauke, B.; Mai, Y.-W. *Science and Engineering of Short Fibre Reinforced Polymer Composites*; CRC Press: Berlin/Heidelberg, Germany, 2009.
241. Sanchez-Palencia, E. *Non-Homogeneous Media and Vibration Theory*; Springer: Berlin/Heidelberg, Germany, 1980.
242. Eshelby, J.D. The determination of the elastic field of an ellipsoidal inclusion, and related problems. Proc. Math. Phys. Eng. Sci. 241: 376–396, 1957.
243. Shin, H.; Choi, J.; Cho, M. An efficient multiscale homogenization modeling approach to describe hyperelastic behavior of polymer nanocomposites. *Compos. Sci. Technol.* **2019**, *175*, 128–134.
244. Mei, C.C.; Vernescu, B. *Homogenization Methods for Multiscale Mechanics*; World Scientific Publishers: Hackensack, NJ, USA, 2010.
245. Segurado, J.; Llorca, J. A numerical approximation to the elastic properties of sphere-reinforced composites. *J. Mech. Phys. Solids* **2002**, *50*, 2107–2121.
246. Fritzen, F.; Böhlke, T. Periodic three-dimensional mesh generation for particle reinforced composites with application to metal matrix composites. *Int. J. Solids Struct.* **2011**, *48*, 706–718.
247. Chen, G.; Bezold, A.; Broeckmann, C. Influence of the size and boundary conditions on the predicted effective strengths of particulate reinforced metal matrix composites (PRMMCs). *Compos. Struct.* **2018**, *189*, 330–339.
248. Kanit, T.; Forest, S.; Galliet, I.; Mounoury, V.; Jeulin, D. Determination of the size of the representative volume element for random composites: Statistical and numerical approach. *Int. J. Solids Struct.* **2003**, *40*, 3647–3679. https://doi.org/10.1016/S0020-7683(03)00143-4.
249. Savvas, D.; Stefanou, G.; Papadrakakis, M. Determination of RVE size for random composites with local volume fraction variation. *Comput. Methods Appl. Mech. Eng.* **2016**, *305*, 340–358.
250. Majewski, M.; Kursa, M.; Holobut, P.; Kowalczyk-Gajewska, K. Micromechanical and numerical analysis of packing and size effects in elastic particulate composites. *Compos. Part B Eng.* **2017**, *124*, 158–174.
251. Ostoja-Starzewski, M. Scale effects in plasticity of random media: Status and challenges. *Int. J. Plast.* **2005**, *21*, 1119–1160.
252. Kuang, C.L.; Anindya, G. Validity of random microstructures simulation in fiber-reinforced composite materials. *Compos. Part B-Eng.* **2014**, *57*, 56–70.
253. Pivovarov, D.; Zabihyan, R.; Mergheim, J.; Willner, K.; Steinmann, P. On periodic boundary conditions and ergodicity in computational homogenization of heterogeneous materials with random microstructure. *Comput. Methods Appl. Mech. Eng.* **2019**, *357*, 112563.
254. Betsch, P.; Gruttmann, F.; Stein, E. A 4-node finite shell element for the implementation of general hyperelastic 3D-elasticity at finite strains. *Comput. Methods Appl. Mech. Eng.* **1996**, *130*, 57–79.
255. Bessa, M.A.; Bostanabad, R.; Liu, Z.; Hu, A.; Apley, D.W.; Brinson, C.; Chen, W.; Liu, W.K. A framework for data-driven analysis of materials under uncertainty: Countering the curse of dimensionality. *Comput. Methods Appl. Mech. Eng.* **2017**, *320*, 633–667.
256. Liu, Z.; Wu, C. Exploring the 3D architectures of deep material network in data-driven multiscale mechanics. *J. Mech. Phys. Solids* **2019**, *127*, 20–46.
257. Liu, Z.; Wu, C.; Koishi, M. A deep material network for multiscale topology learning and accelerated nonlinear modeling of heterogeneous materials. *Comput. Methods Appl. Mech. Eng.* **2019**, *345*, 1138–1168. https://doi.org/10.1016/j.cma.2018.09.020.
258. Bhattacharjee, S.; Matous, K. A nonlinear manifold-based reduced order model for multiscale analysis of heterogeneous hyperelastic materials. *J. Comput. Phys.* **2016**, *313*, 635–653.
259. Yvonnet, J.; He, Q.-C. The reduced model multiscale method (R3M) for the non-linear homogenization of hyperelastic media at finite strains. *J. Comput. Phys.* **2007**, *223*, 341–368.

260. Yvonnet, J.; Monteiro, E.; He, Q.-C. Computational homogenization method and reduced database model for hyperelastic heterogeneous structures. *Int. J. Multiscale Comput.* **2013**, *11*, 201–225.
261. Wu, C.; Koishi, M. Three-dimensional meshfree-enriched finite element formulation for micromechanical hyperelastic modeling of particulate rubber composites. *Int. J. Numer. Methods Eng.* **2012**, *91*, 1137–1157.
262. Triantafyllidis, N.; Aifantis, E.C. A gradient approach to localization of deformation. I. Hyperelastic materials. *J. Elast.* **1986**, *16*, 225–237.
263. de Geus, T.; Vondřejc, J.; Zeman, J.; Peerlings, R.; Geers, M. Finite strain FFT-based non-linear solvers made simple. *Comput. Methods Appl. Mech. Eng.* **2017**, *318*, 412–430.
264. Michel, J.C.; Suquet, P. Computational analysis of nonlinear composite structure using the non-uniform transformation 3field analysis. *Comput. Methods Appl. Mech. Eng.* **2004**, *193*, 5477–5502.
265. Ehlers, W.; Bidier, S. From particle mechanics to micromorphic media. Part I: Homogenisation of discrete interactions towards stress quantities. *Int. J. Solids Struct.* **2018**, *187*, 23–37. https://doi.org/10.1016/j.ijsolstr.2018.08.013.
266. Huang, Z.P.; Wang, J. A theory of hyperelasticity of multi-phase media with surface/interface energy effect. *Acta Mech.* **2006**, *182*, 195–210.
267. Jahanshahi, M.; Ahmadi, H.; Khoei, A. A hierarchical hyperelastic-based approach for multi-scale analysis of defective nano-materials. *Mech. Mater.* **2019**, *140*, 103206.
268. Masud, A.; Truster, T.J. A framework for residual-based stabilization of incompressible finite elasticity: Stabilized formulations and F methods for linear triangles and tetrahedra. *Comput. Methods Appl. Mech. Eng.* **2013**, *267*, 359–399.
269. Bisegna, P.; Luciano, R. Bounds on the overall properties of composites with debonded frictionless interfaces. *Mech. Mater.* **1998**, *28*, 23–32.
270. Dai, M.; Schiavone, P.; Gao, C.-F. Neutral nano-inhomogeneities in hyperelastic materials with a hyperelastic interface model. *Int. J. Non-Linear Mech.* **2016**, *87*, 38–42.
271. Wang, X.; Schiavone, P. Harmonic three-phase circular inclusions in finite elasticity. *Contin. Mech. Thermodyn.* **2015**, *27*, 739–747.
272. Wang, X.; Schiavone, P. Neutral coated circular inclusions in finite plane elasticity of harmonic materials. *Eur. J. Mech. A/Solids* **2012**, *33*, 75–81.
273. Ma, J.; Sahraeem, S.; Wriggers, P.; de Lorenzis, L. Stochastic multiscale homogenization analysis of heterogeneous materials under finite deformations with full uncertainty in the microstructure. *Comput. Mech.* **2015**, *55*, 819–835.
274. Sasikumar, P.; Suresh, R.; Gupta, S. Stochastic model order reduction in uncertainty quantification of composite structures. *Compos. Struct.* **2015**, *128*, 21–34.
275. Kamiński, M. Sensitivity and randomness in homogenization of periodic fiber-reinforced composites via the response function method. *Int. J. Solids Struct.* **2009**, *46*, 923–937.
276. Ma, J.; Temizer, I.; Wriggers, P. Random homogenization analysis in linear elasticity based on analytical bounds and estimates. *Int. J. Solids Struct.* **2011**, *48*, 280–291.
277. Kamiński, M. Gaussian uncertainty in homogenization of rubber–carbon black nanocomposites. *Compos. Struct.* **2014**, *113*, 225–235.
278. Kamiński, M.; Lauke, B. Parameter sensitivity and probabilistic analysis of the elastic homogenized properties for rubber filled polymers. *CMES Comput. Model. Eng. Sci.* **2013**, *93*, 411–440.
279. Kamiński, M.; Lauke, B. Probabilistic homogenization of polymers filled with rubber particles. *Comput. Mater. Sci.* **2014**, *82*, 483–496.
280. Kamiński, M. Multiscale homogenization of n-component composites with semi-elliptical random interface defects. *Int. J. Solids Struct.* **2005**, *42*, 3571–3590.
281. Sokołowski, D.; Kamiński, M. Probabilistic homogenization of hyper-elastic particulate composites with random interface. *Compos. Struct.* 2020, 241,112118.
282. Sokołowski, D.; Kamiński, M.; Wirowski, A. Energy fluctuations in the homogenized hyper-elastic particulate composites with stochastic interface defects. *Energies* **2020**, *13*, 20112020.
283. Allaix, D.; Carbone, V. An improvement of the response surface method. *Struct. Saf.* **2011**, *33*, 165–172. https://doi.org/10.1016/j.strusafe.2011.02.001.
284. Rajashekhar, M.R.; Ellingwood, B.R. A new look at the response surface approach for reliability analysis. *Struct. Saf.* **1993**, *12*, 205–220. https://doi.org/10.1016/0167-4730(93)90003-J.
285. Jurecka, F.; Ganser, M.; Bletzinger, K.U. Update scheme for sequential spatial correlation approximations in robust design optimization. *Comp. Struct.* **2007**, *85*, 606–614.
286. Simpson, T.W.; Poplinski, J.D.; Koch, P.N.; Allen, J.K. Metamodels for Computer-based Engineering Design: Survey and recommendations. **Eng. Comput. 2001**, *17*, 129–150. https://doi.org/10.1007/PL00007198.
287. Draper, N.; Smith, H. *Applied Regression Analysis*; Wiley: New York, NY, USA, 1998.
288. Myers, R.H.; Montgomery, D.C. *Response Surface Methodology, Process and Product Optimization Using Designed Experiments*, 2nd ed.; Wiley: New York, NY, USA, 2002.
289. Alibrandi, U.; Impollonia, N.; Ricciardi, G. Probabilistic eigenvalue buckling analysis solved through the ratio of polynomial response surface. *Comput. Methods Appl. Mech. Eng.* **2010**, *199*, 450–464. https://doi.org/10.1016/j.cma.2009.08.015.
290. Settineri, D.; Falsone, G. An APDM-based method for the analysis of systems with uncertainties. *Comput. Methods Appl. Mech. Eng.* **2014**, *278*, 828–852. https://doi.org/10.1016/j.cma.2014.06.014.

291. Dantzig, G.B. *Linear Programming and Extensions*; Princeton University Press: Princeton, NJ, USA, 1963.
292. Lemke, C.E. The dual method of solving the linear programming problem. *Nav. Res. Logist. Q.* **1954**, *1*, 36–47.
293. Forrest, J.J.H.; Tomlin, J.A. Vector processing in simplex and interior methods for linear programming. *Ann. Oper. Res.* **1990**, *22*, 71–100.
294. Boland, N. A dual-active-set algorithm for positive semi-definite quadratic programming. *Math. Program.* **1996**, *78*, 1–27.
295. Gould, N.I.M.; Toint, P.L. An iterative working-set method for large-scale non-convex quadratic programming. *Appl. Numer. Math.* **2002**, *43*, 109–128.
296. Monteiro, R.D.C.; Adler, I. Interior path following primal-dual algorithms, Part II: Convex quadratic programming. *Math. Program.* **1989**, *44*, 43–66.
297. Vanderbei, R.J. LOQO:an interior point code for quadratic programming. *Optim. Methods Softw.* **1999**, *11*, 451–484.
298. Wright, M.H. Interior methods for constrained optimization. *Acta Numer.* **1992**, *1*, 341–407.
299. Gill, P.E.; Murray, W.; Ponceleón, D.B.; Saunders, M.A. *Solving Reduced KKT Systems in Barrier Methods for Linear and Quadratic Programming*; Report SOL 91-7; Department of Operations Research, Stanford University: Stanford, CA, USA, 1991.
300. Gill, P.E.; Murray, W.; Saunders, M.A.; Tomlin, J.A.; Wright, M.H. Wright, On projected Newton barrier methods for linear programming and an equivalence to Karmarkar's projective method. *Math. Program.* **1986**, *36*, 183–209.
301. AFiacco, V. Barrier methods for nonlinear programming. In *Operations Research Support Methodology*; Marcel Dekker: New York, NY, USA, 1979; pp. 377–440.
302. Murray, W. Analytical expressions for the eigenvalues and eigenvectors of the Hessian matrices of barrier and penalty functions. *J. Optim. Theory Appl.* **1971**, *7*, 189–196.
303. Vavasis, S.A. *Nonlinear Optimization: Complexity Issues*; Oxford University Press: Oxford, UK, 1991.
304. Wu, C.; Tau, X.C. Augmented lagrangian method, dual methods, and split Bregman iteration for ROF, Vectorial TV, and High Order Models. *SIAM J. Imaging Sci.* **2010**, *3*, 330–339.
305. Forsgren, A.; Gill, P.E.; Wright, M.H. Interior Methods for Nonlinear Optimization. *SIAM Rev.* **2002**, *44*, 525–597.
306. Diehl, M.; Ferreau, H.J.; Haverbeke, N. *Efficient Numerical Methods for Nonlinear MPC and Moving Horizon Estimation*; Springer: Berlin/Heidelberg, Germany, 2009; pp. 391–417.
307. Lasdon, L.S.; Waren, A.D.; Jain, A.; Ratner, M. Design and testing of a generalized reduced gradient code for nonlinear programming. *ACM Trans. Math. Soft.* **1978**, *4*, 34–50.
308. Gabriele, G.A.; Ragsdell, K.M.The generalized reduced gradient method: A reliable tool for optimal design. *J. Eng. Ind.* **1977**, *99*, 394–400.